An Investigation of Cornice Development Control at Kvannberget, Norway

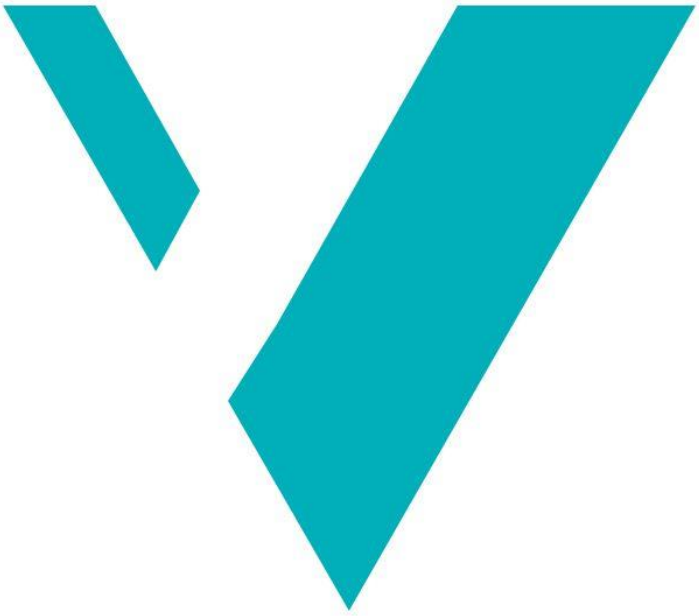

Åsmund Skancke Karlsnes

Master Thesis in Climate Change Management

Department of Environmental Sciences, Faculty of Engineering and Science

WESTERN NORWAY UNIVERSITY OF APPLIED SCIENCES

Sogndal

December, 2020

Western Norway University of Applied Sciences

An Investigation of Cornice Development Control at Kvannberget, Norway

Master thesis in Climate Change Management

Author: Åsmund Skancke Karlsnes	Author sign. Åsmund Skancke Karlsnes
Thesis submitted: Autumn 2020	Confidential thesis
Main Supervisor: Simon De Villiers Co-supervisors: Markus Eckerstorfer	
Keywords: Snow Cornice, Meteorological controls, Mitigation Measures, Wind baffles, Climate Change	Number of pages: 68 + Appendix: 0 Sogndal, 15.12, 2020 Place/Date/year

This thesis is a part of the master's program in Climate Change Management (Planlegging for klimaendringer) at the Department of Environmental Sciences, Faculty of Engineering and Science at the Western Norway University of Applied Sciences. The author(s) is responsible for the methods used, the results that are presented and the conclusions in the thesis.

Western Norway University of Applied Sciences

Preface

To my classmates, students, teachers and friends associated with the master program, thank you for making this period of my life a memorable one.

A special thanks to Simon De Villiers, for all the discussions and help along the way. Without you towing me on skis up to Kvannberget this would not be possible.

Thank you to; Stian Langeland at Wyssen for providing me with the opportunity to write this thesis; Markus Eckerstorfer for the insights shared; Sigurd Daniel Nerhus for helping me with the installation of the monitoring equipment; Hydro for transporting me and the equipment up to the field site; and all the students in the HVL cantina for the necessary breaks during the writing process.

Figure 0-1: The view from Kvannberget during field work in October. Fortunsdalen below.

Western Norway University of Applied Sciences

Abstract

Snow cornices develop along mountain ridges and plateaus in areas with seasonal snow cover and are recognized as a natural hazard endangering life and infrastructure in mountainous areas. At Kvannberget, Western Norway, the horizontal extent of a large continuous cornice has previously interfered with power lines that transport electricity from hydropower installations above Fortunsdalen. In 2019 five wind baffles were installed at the location to permanently mitigate the hazard posed by the cornice structure.

During the 2019/2020 winter season the area previously subject to the development of a large continuous snow cornice, as well as a reference cornice, was monitored using time-lapse imagery and an automatic weather station (AWS). The temporal resolution of the images capturing cornice development and local meteorological data acquired, enabled detailed observation of cornice accretion events, analysis of the meteorological controls of cornice accretion, and a visual evaluation of the effectiveness of the installed wind baffles.

The results of the investigations provide reinforcement to the existing conceptual models of cornice development. Cornice accretion at Kvannberget is a response to distinct meteorological events: North-Easterly winds with hourly wind speed averages of 10 m/s and temperatures below 0°C, with snow available for transport. The local wind regime at Kvannberget deviates from the wind regime at the meteorological station at Sognefjellet and accretion events are likely connected to local fall winds. Cornice accretion rates of up to 46mm/hour were observed, significantly higher than measurements made in previous studies.

Cornice accretion events could become more frequent in a future climate with increased winter precipitation and wind speeds if the average winter temperature remains below freezing. The wind baffles effectively mitigated the development of a continuous cornice and prove to be proficient as a cornice mitigation measure in areas with a prevailing wind direction, although the effectiveness of 2 of the baffles could be optimized with a more ridge ward placement.

Western Norway University of Applied Sciences

Sammendrag

Snøskavler dannes langs fjellrygger og fjellplatå i områder med snødekke. Skavler er en kjent naturfare og kan utgjøre en risiko for mennesker og infrastruktur i fjellområder. Vest i Norge, på Kvannberget, har den horisontale utstrekningen til en stor sammenhengende snøskavl tidligere skapt problemer ved kraftlinjene som transporterer strøm fra vannkraftanlegg i fjellområdene øst for Fortunsdalen. I 2019 ble det installert fem snøskjermer for å hindre skavldannelse i det tidligere problemområdet.

Gjennom vintersesongen 2019/2020 ble det tidligere problemområdet, i tillegg til en referanseskavl, overvåket ved hjelp av time-lapse bildeserier og en automatisk værstasjon. Den hyppige datainnsamlingen muliggjorde en detaljert kartlegging av skavlutvikling og de tilhørende lokale værforholdene, samt en visuell evaluering av effekten av snøskjermene.

Resultatene fra Kvannberget underbygger de eksisterende modellene for skavlutvikling. Skavldannelse på Kvannberget skjer som en respons på spesifikke lokale værforhold: Det må være snø tilgjengelig for transport, temperaturer under 0°C, og vind dra Nord-Øst med en gjennomsnittlig hastighet rundt 10 m/s. De lokale vindforholdene på Kvannberget avviker fra vindforholdene målt på værstasjonen på Sognefjellet, og skavlvekst skjer sannsynligvis på grunn av lokale fallvinder. Skavlen hadde en maksimum vekstrate på 46mm/time, som er mye høyere enn målinger gjort i tidligere studier.

Økt vinternedbør og høyere vindhastigheter kan føre til at skavldannelse blir mer utbredt i et fremtidig varmere klima, hvis temperaturene forblir under frysepunktet. Snøskjermene hindret dannelsen av en sammenhengende skavl og viste seg å være et tilstrekkelig sikringsmiddel i områder med en dominerende vindretning. Effekten til 2 av snøskjermene kunne vært forbedret med en plassering nærmere kanten på platået.

List of Figures

1 Introduction

1.1. Motivation and scope of the study

Snow cornices are a natural hazard that put people and infrastructure at risk in mountainous areas. The West facing ridgeline at Kvannberget is prone to the development of a large, continuous cornice structure. Contrary to other locations, where cornice fall and resulting snow avalanches are the most pronounced threats posed by snow cornices (Montagne, McPartland, Super, & Townes, 1968), the problem at Kvannberget is connected to the horizontal extent of the cornice and the power lines coming in contact with the snow surface.

In 2018, temporary mitigation work, in the form of explosives, was conducted to reduce the horizontal extent of the cornice. Active control measures used to mitigate snow related hazards, e.g. explosives, require significant personnel resources, without a guarantee for a positive outcome (Hewes, Decker, Wood, & Jamie Yount, 2008). Passive defense measures have the potential to cost-effectively reduce hazards without the need for personnel and permanently mitigate hazards (Hewes et al., 2008). In 2019 five wind baffles were erected to hinder cornice development at the site. Wind baffles are common in the Alps (Hákonardóttir, Margreth, Tómasson, Indriðason, & Thordarson, 2008) but have, to knowledge of the author, rarely been used in Norway.

Previous research on cornice formation has been limited (Eckerstorfer & Vogel, 2014) and based of the observations of cornices in a few selected areas (e.g. Kobayashi, Ishikawa, & Nishio, 1988; Montagne et al., 1968; Vogel, Eckerstorfer, & Christiansen, 2012). Snow cornice development is a function of a complex interaction between terrain, snowpack and meteorological conditions (Vogel et al., 2012). The development of cornice structures is directly linked to snow cover characteristics and is strongly influenced by meteorological conditions, e.g. air temperature, precipitation and wind conditions (Vogel et al., 2012). Consequently it is likely that cornice development will be affected by the documented effects of current and future climate change. Snow commonly occurs in mountainous environments where the temperature is close to the 0°C isotherm and should respond quickly to climatic fluctuations (Germain, Filion, & Hétu, 2009).

The aim of the thesis is to investigate the meteorological controls of cornice growth at Kvannberget, evaluate the effectiveness of the installed wind baffles and discuss how climate change can affect future cornice development. This will be achieved through: An in depth literature review on cornice formation and meteorological conditions conducive of growth; A review of snow drift control measures with a focus on the effectiveness of wind baffles; A review of future projected changes in meteorological conditions relevant to cornice development at Kvannberget, and; Monitoring of meteorological conditions and cornice development through installation of an automatic weather station and time-lapse cameras at Kvannberget.

Figure 1-1: The horizontal extent of the cornice structure at Kvannberget has previously interfered with the power lines. Note the small depression at the lip of the cornice where the powerline from the second mast from the left was been in contact with the snow. The image is from 2018.

1.2. Cornice Theory

1.2.1 Cornices

A cornice can be defined as a wedge-shaped, overhanging deposit of wind drifted snow that projects over the top of a rock or ice face (Montagne et al., 1968). Cornices form on the lee side of abrupt changes in slope angle due to the differences in air flow (McClung & Schaerer, 2006). Cornices consists of wind packed snow and can have a density of up to 500kg/m3 (McClung & Schaerer, 2006).

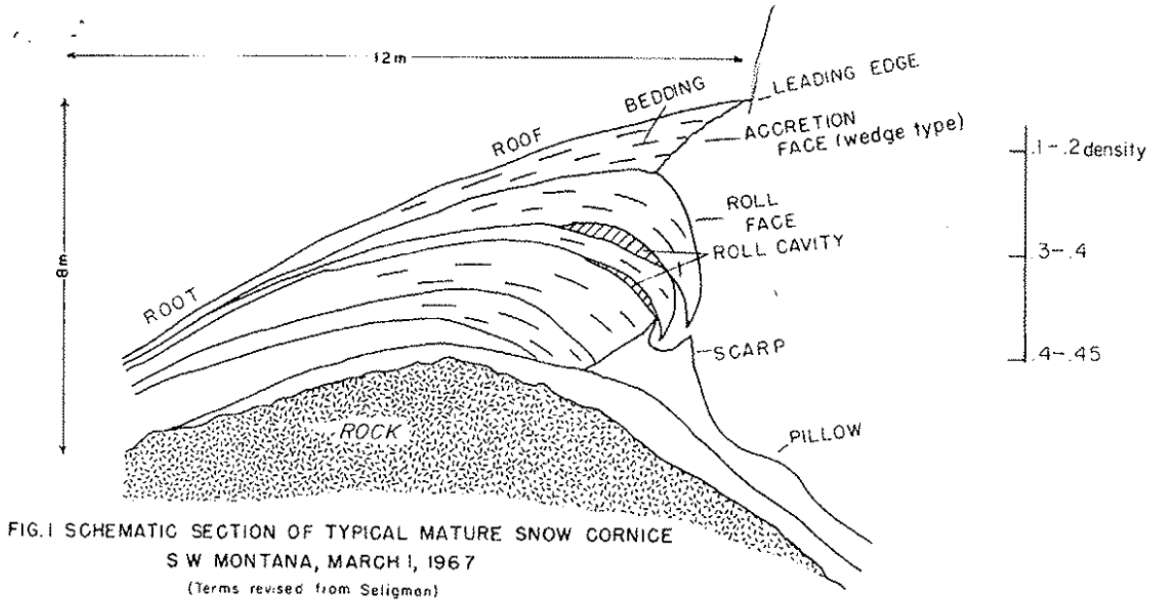

Figure 1-2: Cross section of a typical cornice structure. The roof of the cornice connects the root on the windward to the cornice root at the lee side of the structure. (Montagne et al., 1968)

The cornice structure is separated into different sections termed the root, the roof and the face (**Figure 1-2**). The root connects the cornice mass to the snow cover on the ridge or mountainside. The cornice face is the leeward side of the cornice. The root and the face are connected by the surface layer of the cornice termed the cornice roof (Seligman, 1936). The cornice face can be subdivided into the leading edge, the roll face and the accretion face (Montagne et al., 1968). Underlying a cornice on the leeward slope a steep-fronted deposit of wind-drifted snow is often found called the scarp (Seligman, 1936). The undisturbed snow further down the leeward slope connects to the scarp via the pillow.

1.2.2 Topography

Ridgelines are common locations for cornice formation due to sharp changes in inclination (Seligman, 1936). Cornices are mostly formed perpendicularly to the ridgeline (Kobayashi et al., 1988) because of differences in upper layer and surface wind direction. Through investigations in Japan, Kobayashi et al. (1988) suggested that surface winds choose the shortest routes when flowing up a mountain slope which is perpendicular to the ridge line, leading to enhanced snow drift conducive of cornice accretion.

Cornices can grow both horizontally and vertically and the shape, size and extent is widely determined by the underlying terrain. The horizontal projection of a cornice is limited by the declivity of the leeward slope. If the declination exceeds 35° the cornice cannot grow to a large horizontal extent due to the narrow support offered by the lee slope. Depending on where they grow cornices can be separated into different types based on the topographical location, e.g. ridge vs. plateau.

The size of cornices is also dependent on the size of the source area on the windward side and the inclination of the slope from the source area to the area of deposition. The slope angle on the windward side of the slope and the overall change in slope angle are determining factors of whether a snowdrift or cornice will form (McClung & Schaerer, 2006). An inclination between 16°-40° is most favorable (Seligman, 1936). If the predominant wind direction blows perpendicularly towards a steep edge, passing over large source area, the resulting cornice can become very large.

1.2.3 Formation

Cornices consist of alternating layers of dense and less dense snow originating from different weather events (Welzenbach and Paulcke, cited in Seligman, 1936). Some snow particles tend to slow down when passing the crest of a ridge (Seligman, 1936). These particles adhere to the preexisting snow surface and start to form a cornice. The other faster moving particles are transported beyond the ridgeline and deposit on the lee slope below and form the scarp. Wind gauges placed on top of a cornice indicate that the wind speed at leading edge of the cornice is several percent lower than the wind speed at the root of the cornice (Montagne et al., 1968).

The leading edge is constantly deformed giving it a convex shape. The reduction in wind speed is a result of divergence of the air moving over a convex surface (Montagne et al., 1968).

Cornice growth is referred to as cornice accretion to depict the gradual growth of the structure (Montagne et al., 1968). Cornice accretion can be divided into three main types; Wedge accretion, vertical accretion and sheet accretion (Montagne et al., 1968). Wedge accretion is the most common type of growth where wind transported snow deposits on the downwind side of the cornice extending it horizontally and vertically. Sheet accretion depicts the formation of a thin horizontal sheet during snowfall which can horizontally extend 10cm into free air. Vertical accretion depicts growth periods without any horizontal extension of the cornice.

Field experiments show that the formation of a cornice starts with the formation of a wind slab during a snow drifting event (Kobayashi et al., 1988). The wind slab extents towards leeward and collects windblown snow particles continuously on the surface. The upper surface (roof) was observed to be horizontal during drifting events for a cornice with a flat source area but will start to sag downwards due to deformation and the lack of support underneath when the drifting stops (Kobayashi et al., 1988). The lower surface of the cornice is not subject to growth during drifting events (Kobayashi et al., 1988).

In a controlled setting small cornices collect as much as 25-50% of the windblown particles (Kobayashi et al., 1988). This large collection efficiency was found to be due to the snow particles being transported by saltation. Even though the cornice might be saging slightly, the bouncing movement of the snow particles makes it easy for the particles to deposit on the cornice surface. The collection coefficient is more variable in a natural setting. In January, the coefficient was 2%. March had much higher values, up to 50%, due to a larger cornice and increased area for deposition (Kobayashi et al., 1988).

Cornices start developing directly following the first snowfall and continuously grow throughout the entire snow season (Vogel et al., 2012). Accretion can occur at any time throughout the winter season as long as there is snow available for transport, wind speeds exceeding threshold for snow transport and a wind perpendicular to the ridgeline (Hancock, Eckerstorfer, Prokop, & Hendrikx, 2020).

1.2.4 Meteorological controls of cornice formation

Snow transport

Snow transport is a prerequisite for cornice formation. Snow is generally picked up in areas of wind acceleration and deposited in areas with wind deceleration (McClung & Schaerer, 2006). The spatial patterns of snow drift is controlled largely by small-scale wind fields over the surface topography and the surface snow properties (Prokop & Procter, 2016). Local terrain features highly influence surface wind patterns and snow deposition (McClung & Schaerer, 2006). Eddy zones found in the vicinity of an obstacle can cause deposition (Mellor, 1965).

Snow transported close to the surface is termed drifting snow and accounts for around 90% of snow transport (McClung & Schaerer, 2006). Snow drift describes re-distribution of previously deposited snow by wind (Prokop & Procter, 2016). Snow particles transported above a height of around 2m is referred to as blowing snow (McClung & Schaerer, 2006). Wind transport can move large quantities of snow and lee zones can attain amounts that are a factor of three to five times higher than wind protected areas (McClung & Schaerer, 2006).

Snow transport occurs by three different modes (Mellor, 1965). Closest to the snow surface (1-mm depth) dry snow particles are transported by rolling, a creeplike motion (Mellor, 1965). Saltation refers to snow particles bouncing along the surface in a layer with a height of around 10cm. The bouncing particles can dislodge other particles as they impact the snow surface (Mellor, 1965). Saltation occurs when the threshold wind speed is reached (Mellor, 1965).

The threshold wind speed for snow transport is dependent on a number of physical conditions. An increase in temperature and humidity increases the threshold wind speed (McClung & Schaerer, 2006). The threshold wind speed also increases with the time elapsed from deposition due to bond formation between surface particles. The speed of bond formation is dependent on temperature (McClung & Schaerer, 2006). The typical threshold wind speed for loose, unbounded snow is 5 m/s, measured at a 10-m height (McClung & Schaerer, 2006). With a rich source of particles and low surface hardness, e.g. new snowfall, the threshold wind speed will be lower (McClung & Schaerer, 2006).

Deceleration of wind transfers large frictional forces onto the snow surface and these forces set snow particles into movement and lead to snow drift (Statens Vegvesen, 2014). Erosion of the snow surface occurs when the wind speed is high enough on a given surface roughness and the shear stress is large enough to dislodge particles from the surface (Mellor, 1965). The critical shear stress varies with the degree of intergranular bonding and size of snow grains in the surface layers (Mellor, 1965). Therefore, snow surface hardness is very important for ease of drifting (Mellor, 1965). Snow particles that have been transported by wind are mechanically broken down into smaller particles that bond more readily, forming a denser surface layer that requires increased wind speeds to be transported (McClung & Schaerer, 2006).

Wind speeds of a few meters per second may dislodge snow particles in cold, cohesionless, fine-grained snow but is not enough to diffuse the particles into the airstream (Mellor, 1965). These particles will instead move through rolling or saltation (Mellor, 1965). Most drifting therefore occurs during snowfall and the following day or so (Verge & Williams, 1981). Wind speeds over 25 m/s can be necessary to transport snow if the surface is well bonded and dense (McClung & Schaerer, 2006).

Winter in Norway typically has higher wind speeds due to large temperature differences between land and ocean. Fall winds (topographic winds) are typical in Norwegian valleys due to the temperature difference between areas at high altitudes and the bottom of the valleys. In mountainous areas the highest wind speeds are often reached when topographic winds and free air winds move in the same (Statens Vegvesen, 2014).

Findings from earlier studies

Cornice accretion is mainly controlled by storm events with a wind direction perpendicular to the ridgeline and wind speed average above 12m/s at a 3-m height (Vogel et al., 2012). Cornices will form with a wind speed around 5 m/s and up to wind speeds around 25 m/s (McClung & Schaerer, 2006). Vogel et al. (2012) found that cornice accretion occurred when the average hourly wind speed measured was about 8 m/s at a 3-m height. Hancock et al. (2020) observed horizontal accretion rates above 10mm per hour.

Speeds greater than 25 m/s can lead to scouring and degrowth of the cornice structure as the wind scours the root of the cornice (McClung & Schaerer, 2006). The primary transport mode of snow particles at such high wind speeds will be through suspension and most of the snow will be transported to and deposited further down on the leeward slope (McClung & Schaerer, 2006). Winds blowing in the opposite direction, towards the cornice face, with speeds over 30 m/s lead to scouring of the cornice and a reduction in vertical and horizontal mass (Vogel et al., 2012).

1.2.5 Deformation

Cornices start to deform during or shortly after formation (Welzenbach and Paulcke, cited in Seligman, 1936). The leading edge is subject to the largest deformation since it is the thinnest and most unsupported part of the cornice. With sufficient deformation the tip of the leading edge may connect with the underlying surface entrapping an area of air inside the cornice structure. This process is known as involution (Seligman, 1936) and the pocket of air is termed a roll cavity (Montagne et al., 1968). The process is a result of intergranular adjustment and is critical for the stability of the cornice structure (Montagne et al., 1968). Roll cavities act as weakness zones and tend to localize future fractures. Many failures occur along these interfaces which can persist throughout the entire snow season (Vogel, 2010).

Constant creep and glide processes in the cornice structures lead to the formation of tension fractures between the cornice mass and the ridgeline bedrock (Montagne et al., 1968). Initial cracking occurs through distinct changes in air temperatures and significant loading of the cornice structure (Eckerstorfer, Christiansen, Vogel, & Rubensdotter, 2012). The fractures are a result of shear stress developing between the snow pack and the deforming cornice mass (Eckerstorfer et al., 2012).

These processes also lead to the entire cornice mass tilting over time. The cornice mass tilts around a pivot point (Vogel et al., 2012). The temperature at the bottom of a cornice, at the interface between the ground and snow, remains constant throughout most of the winter and the deformation is a result of a constant downwards creep rate rather than changes in air temperature at the pivot point (Eckerstorfer et al., 2012).

Cornices respond rapidly to changes in meteorological conditions and the strength of the structure is critically weakened when the bulk of the cornice mass approaches 0 °C (McCarty, Brown, & Montagne, 1986). The cornice face is the most sensitive to changes in meteorological conditions since it is the most exposed to air temperature (McCarty et al., 1986).

Additional loading, pronounced air temperature changes, rain- on snow events and direct insolation are the main meteorological trigger factors of cornice collapse (Burrows & McClung, 2006). Changes in air temperature and warming of the upper layers of the cornice structure leads to increased rates of creep and weakening of the structure (Eckerstorfer et al., 2012).

1.3. Mitigation Measures

Snowdrift control structures aim to influence snow deposition and the mechanical properties of the snowpack (Rudolf-Miklau, 2015), thereby prevent cornice formation by altering the air flow. The change in airflow affects snow distribution and hardness of the adjacent snow (Hopf & Bernard, 1963). Different types of snow fences, wind roofs and wind baffles (**Figure 1-3**) have been used for this purpose (Perla & Martinelli, 1976). Some structures aim to promote snow deposition in the surrounding area, while others aim to blow snow particles further away. Vortices are generated in the air flow when a wind trajectory meets a snowdrift fence and result in snow deposition. Wind baffles and wind roofs on the other hand increases the wind speed incrementally in their vicinity and snow particles are therefore transported further away (Rudolf-Miklau, Sauermoser, Mears, & Boensch, 2015).

Figure 1-3: Snow fences to the left and wind baffles to the right (Hákonardóttir et al., 2008). Note the increased deposition around the snow fences and the increased erosion around the wind baffles.

1.3.1 Wind baffles

Wind baffles were first introduced in Arlberg, Austria to prevent cornice formation and to aid in avalanche control. These structures set out to create turbulent winds in the vicinity of the baffle and irregular snow deposition. Wind baffles are also called Kolktafeln by the Swiss, which translates to Eddy panel (Wopfner & Hopf, 1963), and parvents by the French (Martinelli, 1960). Wind baffles were based on the experiences gained from the usage of snow fences along roads and railways to prevent snow drifts. The deflection of air caused by the snow fences influenced the morphology of the nearby snow cover. Snow strength/hardness was higher in the proximity of the fences than in undisturbed snow (Hákonardóttir et al., 2008). The idea behind wind baffles was that wind speed increases in the vicinity of the baffle which causes increased snow erosion around the structure. The increased erosion forms a discontinuity in the snow distribution (Hákonardóttir et al., 2008) and the formation of a scour, an eroded snow surface with high surface hardness. The result is a non-uniform snow pack in terms of thickness and density (Rudolf-Miklau et al., 2015).

Wopfner and Hopf (1963) were the first to conduct field studies of wind baffles over several years. The goal was to investigate the effects of different shapes of baffles as well as baffle placement. Experiments were run at two different locations over two winter seasons. One of the locations was at the edge of a plateau were large cornices formed every year due to strong foehn winds. Cornice formation was successfully hindered by the three baffles.

Based on the results of the experiments Hopf and Wopfner recommended that baffles should be placed directly in the cornice root or up to 1m from the edge of the ridge. Two dimensional baffles should be placed perpendicular to the prevailing wind direction. In areas where the prevailing wind direction can not be established cruciform baffles are favorable. The number of baffles and spacing between them is dependent on whether the goal is to entirely prevent cornice formation or if it sufficient to hinder the formation of a large, continuous cornice.

Wind baffles placed side by side can hinder formation of large continuous cornices (Hákonardóttir et al., 2008). Distance between baffles should not exceed baffle width if the goal is to entirely prevent cornice formation. The formation of a 150m long cornice was almost

entirely prevented with baffle spacing of 7-8m in Tschierv, Switzerland (USDA Forest Service, 1975). Four wind baffles failed to reduce the formation of cornices in Iceland (Margreth, Jóhannesson, & Stefánsson, 2014).

The optimal width of a baffle is between 3-4m (Wopfner & Hopf, 1963). Smaller baffles are less efficient and more are needed to reach the same effect. If the baffles are too wide the lateral vortex fields fail to meet, leading to snow accumulation of the downwind side. The baffles should be at least 1m higher that the height of the snow cover, and should therefore be adjusted to the expected snow depths (Wopfner & Hopf, 1963). Wind baffles can either be constructed as a solid structure or with spacing between the boards giving them a lower density. Baffles with a bottom gap of 1-1.2m (Montagne et al., 1968) and a density of 75-80% proved sufficient for preventing cornice formation. Similar results were obtained with different shaped baffles without a bottom gap (Campell, 1955).

A trapezoidal shaped baffle that is wider at the top and narrower at the bottom is advantageous (Campell, 1955; Wopfner & Hopf, 1963). The trapezoidal shape imitates nature, where trees that have bulky branches extended upward have large scours around them. This phenomenon is not found around trees with a more conical shape (USDA Forest Service, 1975). The trapezoidal shaped baffles creates a scour 33% larger than rectangular baffles with the same surface area (USDA Forest Service, 1975). Wind tunnel tests have shown that wind flow pattern is independent of the wind speed (Fuchs, 1954).

1.4. Timelapse photography

Observations of many natural processes are often limited by the timescales they operate on. This is especially true for events that are difficult to predict (Munroe, 2018). Numerous processes in cryosphere research associated in the accumulation and melting of snow are challenging to observe and monitor, such as cornice growth (Kobayashi et al., 1988; McCarty et al., 1986) and collapse (Vogel et al., 2012). Repeat photography was introduced as an observational and monitoring technique to document landscape change (Klett, 2004, 2011; Webb, 1996).

Time-lapse photography is a form of repeat photography where photographs are collected at specific intervals from a fixed location (Malin, 2007). Time-lapse photography was originally developed as a cinematographic technique to replay events at much quicker rates than they occur naturally (van Herwijnen, Berthod, Simenhois, & Mitterer, 2013). The technique has been applied in research to investigate different processes ranging from fluvial geomorphology to cloudiness (Dexter & Cluer, 1999; Holle, Simpson, & Leavitt, 1979), as well as temporal and spatial patterns of snow distributions (Aschenwald, Leichter, Tasser, & Tappeiner, 2001; Parajka, Haas, Kirnbauer, Jansa, & Blöschl, 2012). It benefits from being able to monitor terrain that otherwise would be inaccessible, getting a continuous data record from one location and getting an unbiased, safe observer position (Eckerstorfer, Bühler, Frauenfelder, & Malnes, 2016).

Technological advances have led to increased supply and decreased costs of digital cameras and time-lapse photography has therefore become an inexpensive monitoring technique (van Herwijnen et al., 2013). This has been further supported by the availability of solar powered charging systems and increased battery life. The application range of time-lapse photography is dependent on the image resolution and can vary between a few meters to several hundreds of meters (Eckerstorfer et al., 2016). Temporal resolution depends on the desired application and the time-lapse intervals used.

Time-lapse photography, by the same means as other optical remote sensing technologies, is limited by bad weather conditions. This can result in periods where no usable data is obtained. It also lacks the spatial resolution provided by airborne or satellite-borne remote sensing (Eckerstorfer et al., 2016). Cameras left out in the field are also prone to failure and battery depletion and tend to need supervision in regular intervals (Vogel et al., 2012).

1.4.1 Use in avalanche research

In avalanche research data is often gathered through visual observations from the valley bottom (van Herwijnen et al., 2013). Field based approaches are limited by high-risk exposure, and are often biased towards objects that are easily observed, in easily accessed areas, during stable snow conditions and fair weather (Eckerstorfer et al., 2016). Several remote sensing techniques,

such as radar, seismic or infrasonic monitoring, have been developed to decrease observation limitations (van Herwijnen et al., 2013). Many of these methods are relatively expensive and have not reached the level of reliability needed for operational use (van Herwijnen et al., 2013).

One of the first to monitor snow dynamics using time-lapse photography was Christiansen (2001). Photographs obtained from automatic cameras in combination with snow stakes enabled the production of maps of snow depth and distribution for northeastern Greenland. Time-lapse techniques have become more frequent recently and have been used to monitor cornices, snowbanks and avalanches (Eckerstorfer et al., 2016; Munroe, 2018; van Herwijnen & Fierz, 2014; van Herwijnen & Simenhois, 2012; Vogel et al., 2012). Time-lapse photography has the benefit of providing data with high temporal and spatial resolution enabling correlation between meteorological data and more detailed process understanding (Eckerstorfer et al., 2016).

1.5. Climate Change

Snowfall is dependent on precipitation occurring at sufficiently cold temperatures. Future changes in snowfall are therefore governed by the interplay between changes in precipitation and temperature (Krasting, Broccoli, Dixon, & Lanzante, 2013).In areas where the temperature often is close to zero during winter months, warming may lead to a higher fraction of the total precipitation to fall as rain (Krasting et al., 2013). Colder areas that stay below zero degrees might experience increased snowfall due to higher moisture content in a warmer climate (e.g. Held & Soden, 2006). Decreases in snowfall in the fall and spring can be offset by higher snowfall during the winter months (Krasting et al., 2013).

The mild winters along the west coast of Norway are mainly cause by two factors: Firstly, warm and humid air is transported towards the north through low pressure cells crossing the North Atlantic Ocean, and secondly, the Gulf stream and the northern extension of it, the North Atlantic Current, transports warm seawater from the gulf of Mexico to the Norwegian coast (Laute & Beylich, 2018).

The mean annual air temperature has increased by 1°C from 1900 to 2014 for mainland Norway areas (I Hanssen-Bauer et al., 2017). Mean annual precipitation has increased by 18% since 1900

areas (I Hanssen-Bauer et al., 2017). Wind velocity has increased slightly for the last 50 years areas (I Hanssen-Bauer et al., 2017). The snow season overall has generally been reduced, with smaller amounts of snow in low lying areas and larger amounts of snow in mountainous areas (I Hanssen-Bauer et al., 2017).

The average winter temperature in Sogn og Fjordane is expected to increase with 4°C by 2100 (Norsk Klimaservicesenter, 2017). Annual winter precipitation is expected to increase with 10% (autumn: +15% and spring +10%) (Norsk Klimaservicesenter, 2017). Precipitation during heavy precipitation events is expected to increase with 15% (Norsk Klimaservicesenter, 2017). Mountainous areas might experience increasing amounts of snow towards the middle of the century before increased temperatures will lead to more rainfall (Norsk Klimaservicesenter, 2017). These changes are based on the mean of model runs for RCP 8.5.

The majority, >80% of cases, of winter precipitation maxima on the west coast of Norway are associated with atmospheric river events, where enhanced concentrations of moisture are transported from the tropics to higher latitudes (Whan, Sillmann, Schaller, & Haarsma, 2020). North America, with similar geography and atmospheric flow as the west coast of Norway (Azad & Sorteberg, 2017), receives 30-40% of the total winter precipitation through 1-2 atmospheric river events (Guan, Molotch, Waliser, Fetzer, & Neiman, 2010). There has been a significant increase in the winter maximum five-day precipitation amounts in Northern Europe (Sillmann, Kharin, Zwiers, Zhang, & Bronaugh, 2013). Models and observations show that for the south-west coast (Sogn og Fjordane) atmospheric river events are associated with up to 95% of winter precipitation. The models show that these events will become more frequent and more intense during both summer and winter towards year 2100 (Whan et al., 2020). Future changes in the North Atlantic Oscillation (NAO) may also lead to higher amounts of winter precipitation in Norway (Tsanis & Tapoglou, 2019).

Over time measuring sites, measuring methods and instrumentation has changed significantly which makes it difficult to review long-term wind records (Førland et al., 2016). The influence of local topography provides further difficulties with analysis of wind conditions (Førland et al., 2016). High resolution models are needed in areas with large topographic differences to

effectively describe local wind speeds and (Førland et al., 2016). Lower resolution models are often used, and local wind speed and direction can widely differ from the modeled wind (Førland et al., 2016). Future wind conditions are difficult to model and are affected by systematic error from the global climate as well as from the downscaled regional model (I. Hanssen-Bauer et al., 2015).

Climate models predict that winter winds in Norway will increase in the future for simulations for RCP 4.5 and RCP 8.5 (Hanssen-Bauer et al., 2015). The frequency is shifted towards higher values and maximum values can increase with over 20% (I. Hanssen-Bauer et al., 2015). Ruosteenoja, Vihma, and Venäläinen (2019) found evidence of future increase in frequency of westerly geostrophic winds during winter months of up to 50%.

2 Methods

2.1. Study site

The study site at Kvannberget is located at 960 masl on the edge of a 200m high cliff in Fortunsdalen, Norway. Kvannberget is situated in between Hurrungane and Breheimen at the end of Sognefjorden (Feil! Fant ikke referansekilden.). The area is prone to snowdrifting with winds from the east, leading to the buildup of a large continuous cornice forming at the edge of the cliff.

A power transmission line originating from hydropower stations within the Fortun-Grandfastavassdragene hydropower concession, is redistributed to four different power lines that carry the power westwards down to the power plant in Fortunsdalen. The power lines are supported by 4 masts at the edge of the cliff.

Figure 2-1: Overview of the study site at Kvannberget. Five wind baffles have been placed between the power masts to hinder cornice growth. The power lines extend westwards over the cliff down to the valley bottom in Fortunsdalen. Photo: Wyssen Avalanche Control AG

Five wind baffles are placed in between the masts to mitigate cornice growth (**Figure 2-1**). The installed wind baffles are approximately 4.3m high and 4m wide with trapezoidal shape (**Figure 2-2**). 14 boards, with a height of 21 cm, protrude from 4 sides in the shape of a cross. The

density of the baffle is around 70%. The baffles do not feature a bottom gap. The baffles were numbered from 1 to 5 to ease referencing later in the paper, with 1 being most northward.

The area surrounding the field site is characterized by large differences in elevation, with peaks up to 2405 masl (Store Skagastølstind) and several glaciers. The catchment is largely characterized by a high mountain plateau with an average elevation above 1000 masl. The plateau is undulating and surrounded by high mountain peaks. There are several lakes of various sizes, glaciers and peaks over 1900 masl inside the catchment area.

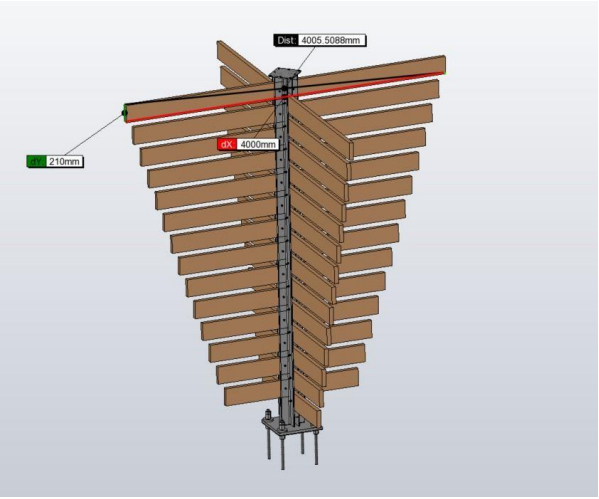

Figure 2-2: Schematic of the installed wind baffles.The width of the longest board is 4m. The baffles do not feature a bottom gap. Photo: Wyssen Avalanche Control AG

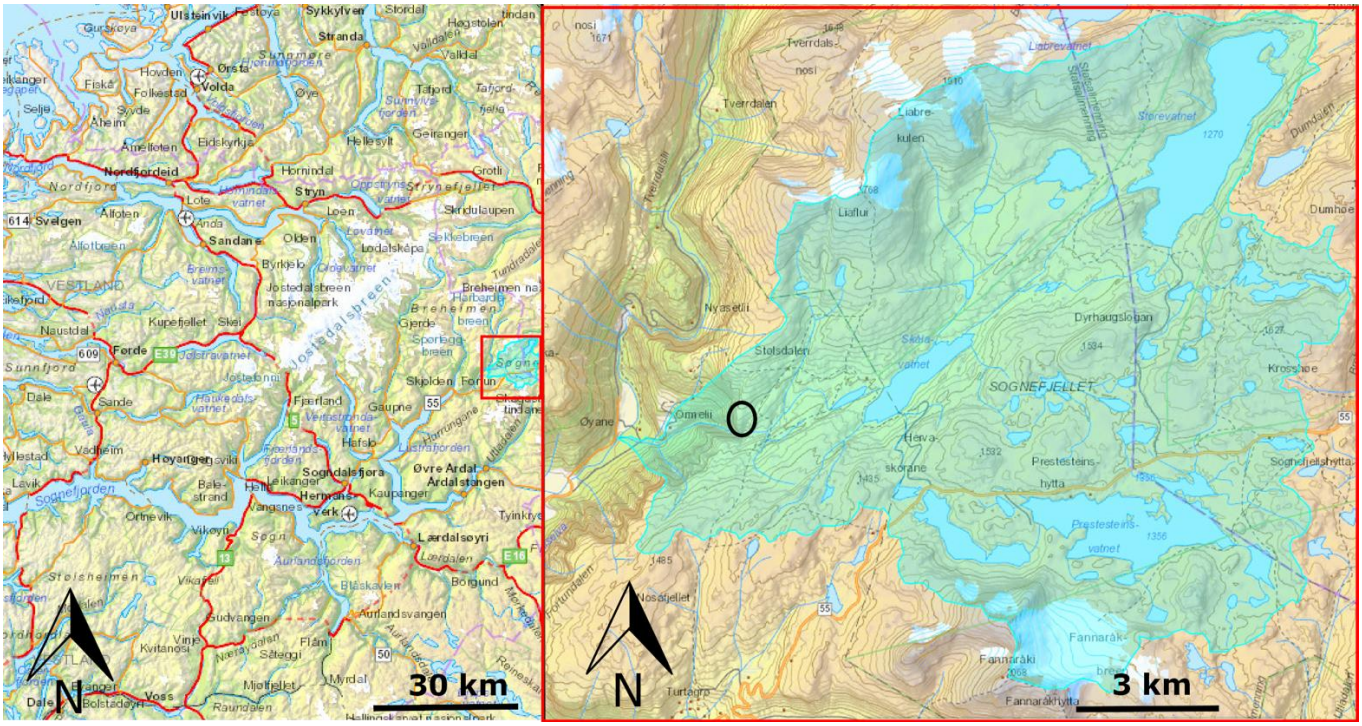

Figure 2-3: A map of the location of the field site at Kvannberget (marked with a black circle) is located in Western Norway on the North-West side of Sognefjorden. The catchment area (shaded in light blue) consists of a mountain plateau to the East of the field site, and several lakes and glaciers. The maps are downloaded from NVE Regine.

2.1.1 Climate

The climate at the study site has continental traits with cold winters and relatively low annual precipitation compared to other regions on the west coast of Norway. There are big regional differences due to the large shifts in elevation and several glaciers in the area. The temperature in the area is affected by the large elevation differences. Fortun has an average July temperature of around 14-15 degrees Celsius, while the average july temperature at Fannaråki, 2068 masl., is around 2-3 degrees Celsius (**Figure 2-4**).

Annual precipitation varies from around 700-800mm along Lustrafjorden to around 2200-2300mm in parts of Breheimen. Interpolated precipitation data from SeNorge indicates that annual precipitation for Kvannberget is in the range of 2000-3000mm. Hurrungane to the south has an annual precipitation of around 1300-1400mm (**Figure 2-4**).

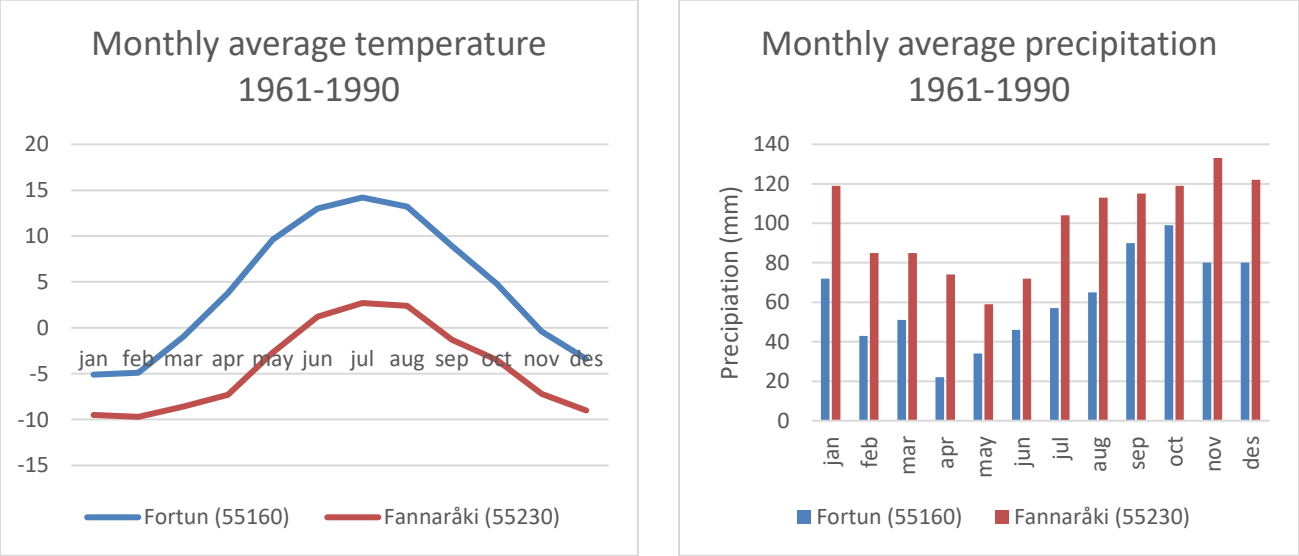

Figure 2-4: Monthly average temperature and precipitation from 1961-1990 from meteorological stations in Fortun (Station nr. 55160) and Fannaråki (Station nr. 55230). (Meteorologisk institutt)

2.2. Fieldwork

The first visit to Kvannberget was conducted on 16.10.19 to install the monitoring equipment. Suitable locations for the cameras and the weather station were chosen based on images of the site from previous winters. Measurement stakes were discarded due to a lack of reliable mounting positions. A fixed object was instead chosen to give relative measures of cornice accretion and snow distribution (see page **24**).

Two more visits on skis were carried out 06.03.20 and 05.05.20 to collect data from the AWS and cameras. The ski tour from Ormeli involved 15km and approximately 1400m of elevation gain and gave insights on cornice formation in the surrounding area. The number of field trips was limited by the length of the tour, lack of daylight and avalanche hazard.

2.3. Meteorological data

2.3.1 Automatic Weather station

Local wind patterns can be very variable over complex terrain (Winstral & marks, 2002) and regional weather stations with longer time series may therefore not provide representative data for the site of interest. Therefore, an Automatic Weather Station (AWS) from Geological Survey of Denmark and Greenland (GEUS) was installed to observe local meteorological data. The weather station is powered by a battery and a 10 W solar panel.

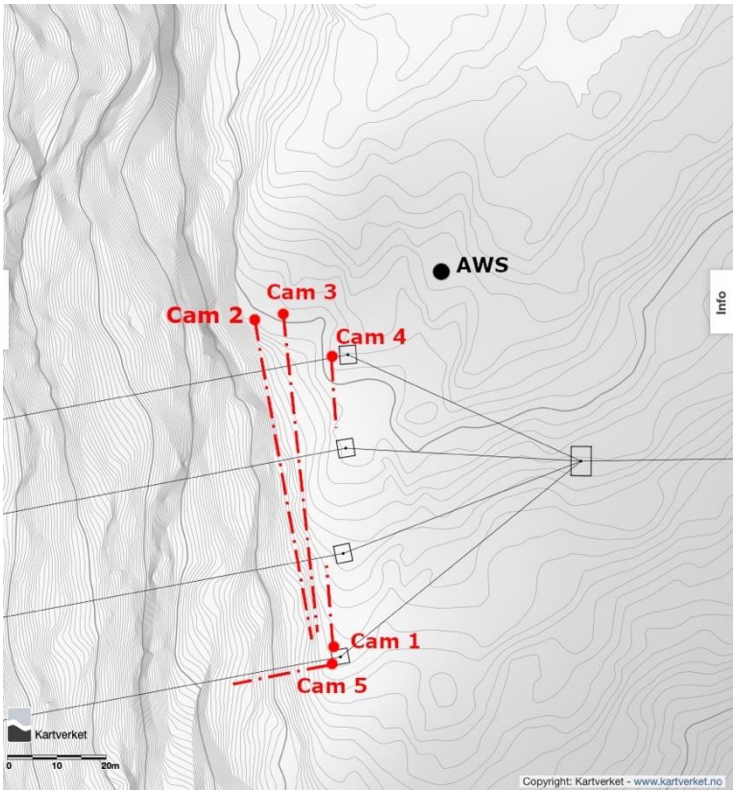

Figure 2-5: Overview of the field site and placement of the AWS (black) and cameras (red). The direction and focus point of the cameras is shown with the dotted red lines. The AWS was placed on an elevated surface to ensure proper wind measurements

The AWS was placed in an area where measurements would not be disturbed by terrain features or obstacles (**Figure 2-5**). The station was placed on a slightly elevated area to prioritize accurate wind measurements, at the cost of accurate snow depth measurements due to more wind erosion (**Figure 2-6**). The location was also chosen to minimize the risk of the AWS being snowed down.

The AWS ran a scan every 10 minutes where all the sensors were powered up and data was saved on the CompactFlash card in the logger. Due to connection issues with the server, the data had to be manually collected from the AWS.

The AWS was primarily used to collect wind observations and temperature at the study site, as well as snow depth and incoming shortwave radiation. Wind data was gathered through the anemometer mounted on the boom of the weather station at a 3.1m height. The anemometer, R.M. Young 05103-5, has a resolution of +-0.3 m/s or 1% and +- 3 degrees in non-riming conditions. It collected average wind speed (m/s) and wind direction (degrees). The height of wind measurements will depend on the snow height. Air temperature was gathered through the Rotronic MP102H with Pt100 and HC2-S3 probe (+- 0.1K, +- 0.8% rh, at 23 degrees Celsius). The 10-min average values were calculated from the last 24 measurements during winter (from day 301 to 99). The AWS did not collect precipitation data.

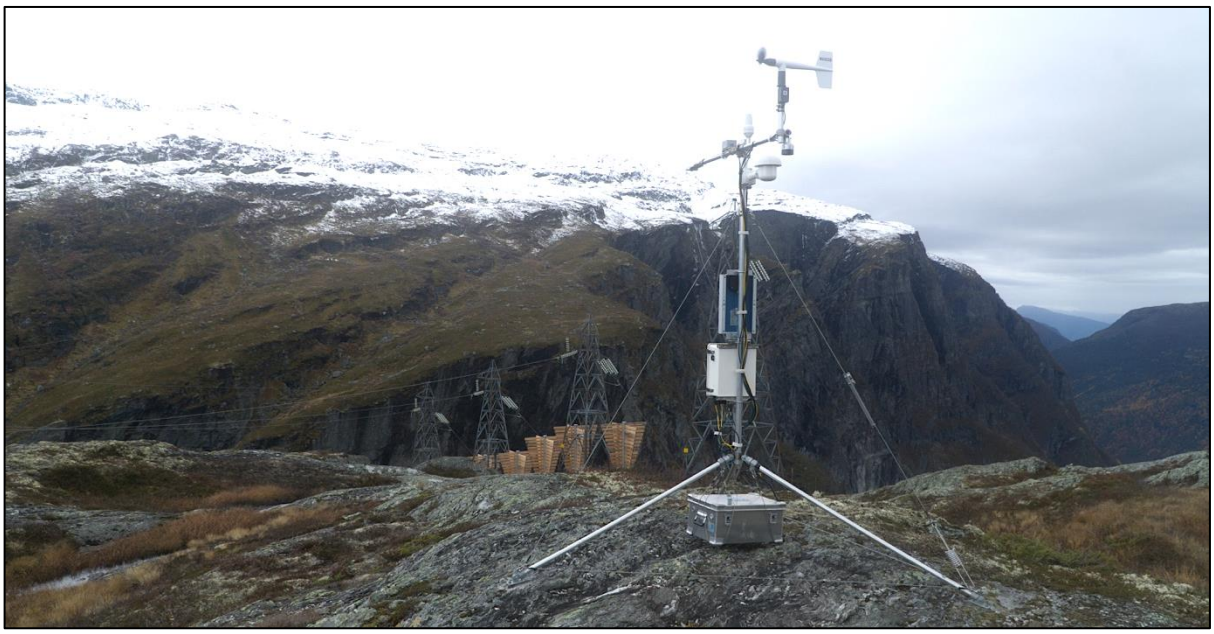

Figure 2-6: The automatic weather station was placed to the Northeast of the wind baffles on an elevated surface. Wind measurements were made at a 3.1m height by the anemometer seen on top of the boom. The boom is mounted in a North-South orientation.

2.3.2 Weather records

Weather records from previous years were downloaded from the Norwegian Meteorological Institute open databases eKlima and SeKlima. Hourly averaged data for temperature, wind speed, wind direction and precipitation were downloaded from station SN55290, Sognefjellshytta, approximately 10,5km to the east. The station is located at 1413 masl, with a measuring record going back to 16.10.2016. Precipitation values from Sognefjellshytta were

used for the field site. The measuring station at Sognefjellshytta will be referred to as Sognefjellet for the rest of the thesis.

2.3.3 Data Analysis

Weather observations were imported into Excel to be sorted and undergo data preparation before being imported into R. The anemometer on the AWS was mounted 180 degrees wrong and the wind directions had to be corrected. 180 degrees was added to all the wind direction measurements. Resulting values above 360 degrees where then subtracted 360 degrees. Wind data from periods where the anemometer froze were manually deleted leading to several periods without data. The measurements of the snow height provided by the AWS was given by the distance from the top of the boom to the ground. The data was transformed to give a more intuitive measurement of snow pack height by subtracting the dataset with the first measurement recorded (the distance from the sensor to bare ground) and then multiplying the data with -1.

The R package openair was used to analyze the weather data. Openair was developed for analysis of air pollution measurement data but can be used for more general purposes in atmospheric sciences (Carslaw & Ropkins, 2012). Data with different measuring intervals were aggregated by creating hourly, daily and monthly averages using the timeAverage function.

Wind direction is reported in polar degrees (0-360) and averaging wind direction is problematic. Simply calculating the arithmetic mean leads to incorrect results, i.e. if a wind is blowing from the north and traverses the discontinuity of the degree scale, the resulting arithmetic mean would show an average wind direction from the southern quadrant. Wind is a vector consisting of a direction and a speed, and trigonometric functions must be used to deal with the discontinuity of polar degree scale. Openair has built in features that correctly process wind data. The wind data was processed using scalar averages.

Generating wind roses to display observations of wind data can introduce directional bias into the data if not handled correctly. The problem arises when wind direction observations are rounded to the nearest 10 degrees and then displayed with angles that is not divisible into e.g. 22.5 degrees. When this data is split into different bins, some angles, e.g. N,E,S,W, will consist of

three intervals while others will consist of two, introducing a significant bias to the plots. Frequency of counts can be overestimated with up to 30% or underestimated with 10% (Droppo & Napier, 2008). Openair handles this issue by globally rescaling the count in each wind direction bin by the number of directions it represents relative to the average.

2.4. Timelapse Cameras

Automatic time lapse cameras were installed to monitor the area that previously had been subject to cornice development, as well as an area where cornice growth was still expected. The cameras that were used was 3x Uovision UV565HD and 2x Uovision UM785-4G (**Table 1**), both with an image resolution of 4000x3000 pixels. These trail cameras were chosen based on battery longevity, weather proofness and timelapse functionality. The images were stored on SD cards on the cameras and had to be manually collected during days of field work.

The functionality and operation time of the cameras during winter was uncertain and therefore a total of five cameras were placed at the site to provide redundancy and different field of views (**Figure 2-5**). Cam 2 and 3 (**Figure 2-7**) were placed on a ridge on the north side of the power lines. These were pointed southwards and gave an overview of the powerlines, wind baffles and the control area. Cam 4 was placed close to the wind baffles to provide detailed images of drifting around the structures. Cam 1 was mounted on the southernmost mast pointing to the North. The last camera, Cam 5, was mounted on the same mast with a field of view towards West.

Figure 2-7: Two cameras were placed on a ridge to the North of the wind baffles and provide a view over the area previously subjected to cornice growth, as well as the control area. The cameras were pointing southwards.

Two of the cameras, the Uovision UM785-4G, had the ability to send pictures over the cellular network through 2-way communication. An external antennae was attached to these cameras to increase reception **(Figure 2-8**). The camera settings could be remotely controlled through a cloud service called LinckEazi Cloud. Image intervals were altered during the monitoring period to ensure that the cameras were operating during hours of daylight and not wasting battery during periods without daylight. Cellular coverage in the area was rather poor and two different operators were used as a test to which functioned best. Real time images (**Figure 2-8**) could be sent through the cloud service and this feature was regularly used to ensure that the cameras were functioning properly.

Figure 2-8: Left: The Uovision UM785-4G with external antennae to increase reception. Right: Example of an image downloaded through the cloud service. This feature was used several times to check if the cameras were operating normally.

Table 1: Configurations of the five different trail cameras used at the field site. Two of the cameras were connected to the 4G-network and could be accessed through a cloud service. External batteries were installed on the cameras deemed most important.

	Cam 1	Cam 2	Cam 3	Cam 4	Cam 5
Camera Type	Uovision UM785-4G	Uovision UM785-4G	Uovision UV565HD	Uovision UV565HD	Uovision UV565HD
Timelapse Interval	2 hours, 05-24	2 hours, 05-24	1 hour, 00-24	2 hours, 05-24	2 hours, 05-24
Network	Telia	Telenor	-	-	-
External Battery	12 AH	12 AH	-	7.5 AH	-

2.5. Image Analysis

The known width of the wind baffles was used as reference to determine accretion rates (**Figure 2-9)**. The focal length and size of the image sensor of the cameras were not known and a reference object had to be used. A pixel per metric ratio was calculated for the width of the baffle (B_w) using the image processing package Fiji (ImageJ). This ratio was then used to calculate the width of one of the supporting beams (BM_1) on the mast directly behind the baffle. The pixel length of the equivalent beam on the mast in the control area (BM_2) was then measured. Knowing that the beams had the same length, a ratio between the measurements could be calculated providing a new pixel per metric ratio in the control area. This ratio was used to calculate the approximate accretion rates during the accretion event 29.02-01.03.20. The method does not take radial and tangential lens distortion into consideration, affecting the accuracy of the rates.

Figure 2-9: Example of the workflow in ImageJ for determining accretion rates by using the known width of the baffle (Bw) and two objects of the same width (Bm). Radial and tangential lens distortion was not accounted for.

To determine the development of the cornice in the control area, the images from the trail cameras were analyzed. Image analysis consisted of 5 steps:

1. Manually identify that the cornice is clearly visible, and that image quality is sufficient for pixel measurement. Images with limited visibility were discarded (**Figure 2-10**). This includes images taken in the dark, in foggy conditions, during snowfall and some periods with snowdrift. On bright and sunny days the automatic white balance on the camera failed at times leading to overexposed pictures. These pictures were also discarded.
2. Compile images into time-lapse animation using Windows Movie Maker to get an overview of snow conditions and cornice development throughout the observation period. Timestamps of different events were noted, i.e. accretion, precipitation, snow drift, increase in snow depth.
3. Analyze vertical and horizontal displacement of the leading edge of the cornice. The images were imported to Fiji (ImageJ). To ensure accurate measurements a macro script was written to crop the images to the same size and add prefixed reference lines. Displacement was measured perpendicularly from the tip of the leading edge to the horizontal and vertical reference line using the line and measurement tool in Fiji (**Figure 2-11**). Displacement was measured in pixels.
4. Measurements and horizontal displacement were timestamped and imported into the weather dataset from the AWS. The data was then analyzed using the openair package in R.
5. Shifts in position due to a new leading edge developing on the cornice structure were removed. A data threshold of minimum displacement of 5 pixels was chosen.

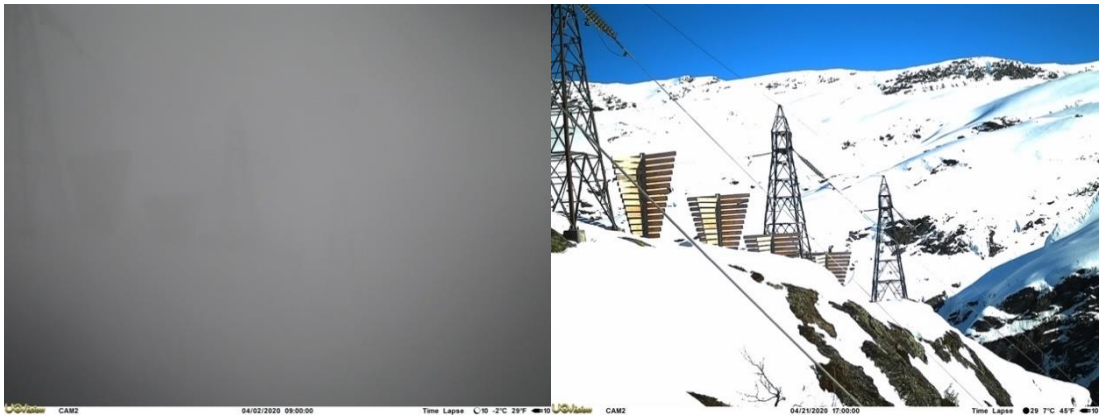

Figure 2-10: Examples of pictures that had to be removed during manual identification. Foggy conditions 04.02.20 on the left and an overexposed picture from 21.04.20 on the right.

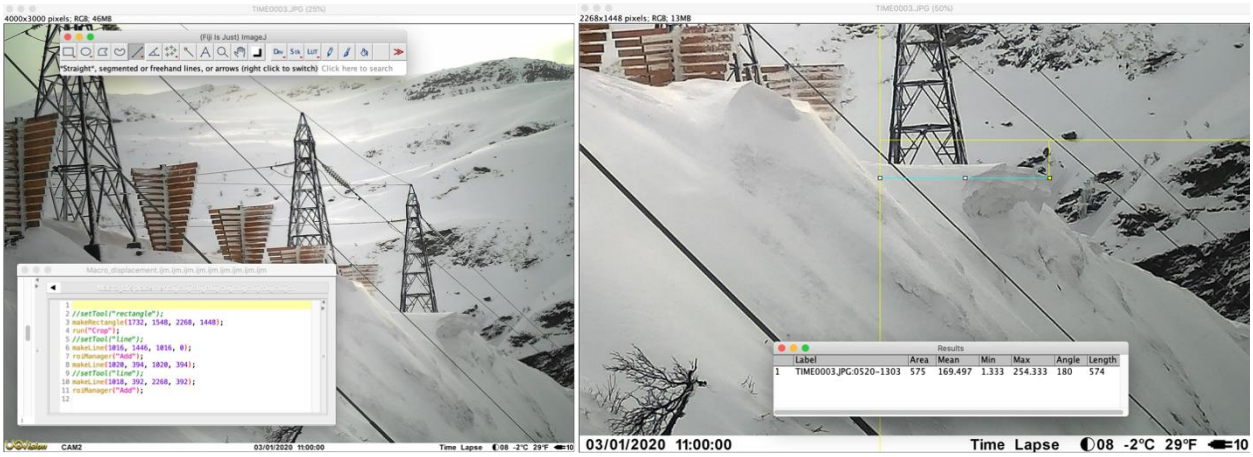

Figure 2-11: Example of workflow in ImageJ. A macroscript was used to draw reference lines. Displacement of the leading edge was measured perpendicularly from these reference lines using the line and measurement tool.

06.03.20 fieldwork was conducted and this included extracting photographs and replacing batteries in the cameras. Camera placement and field of view was slightly altered and the macroscript for measurement had to be adjusted accordingly.

Weather conditions during accretion

To analyze weather conditions during periods of accretion, 5 hour and 24 hour averages preceding the accretion events were calculated. A 5 hour step was chosen to represent the typical meteorological conditions during an event. The 24 hour average was chosen to see how daily averages affect accretion.

Due to the 2 hour image intervals and periods without visibility accretion events could not be timestamped precisely. Given the temporal gap between images it is not possible to determine whether an observed cornice accretion represents a single event drift event, or a composite of multiple drift events closely spaced in time. Hourly data from the AWS connected to images where drifting was clearly visible were investigated to more precisely determine meteorological conditions that led to drifting events and cornice accretion. Events that could be timestamped within 2 hours were also investigated.

3 Results

3.1. Analysis of weather data

A total of 29084 observations of 10-minute data was collected by the AWS. 1881 recordings of 10-min wind speed and direction had to be removed due to faulty observations of wind speed and a locked direction. The recorded wind speed was 0 m/s with a constant wind direction, implying that the anemometer was stuck a fixed direction. Relative humidity was >95% at the start of these periods in combination with decreasing temperatures, conditions that could lead to the anemometer being frozen. Failure of the anemometer coincided with faulty observations of snow depth.

The hourly average temperature from 16.10.2019-05.05.2020 was -2.6° C, with a maximum temperature of 7.1° C (06.04.2020) and minimum of -12.1°C (14.03.2020). Daily average temperature started dropping at the end of November and stayed below freezing until the end of April, with a few exceptions. In total there was 36 days with an average daily temperature above freezing (**Figure 3-1**). The coldest daily temperature was measured 11.11.2019. February was the coldest month with an average temperature of -4.1° C and the month with the highest amount precipitation, due to two days with >10mm precipitation. Precipitation measurements from Sognefjellet were only available until the middle of March (**Figure 3-13**).

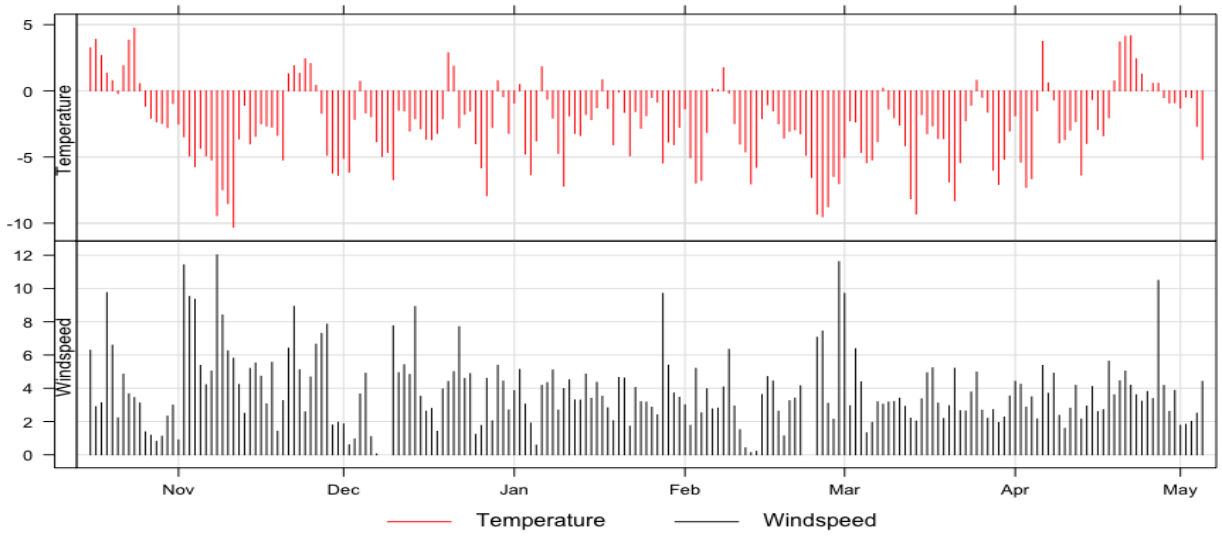

Figure 3-1: Daily average temperature (red) and wind speed (black) data from the AWS. The temperature started dropping at the end of November and mainly stayed below freezing to the start of April. The hourly average temperature was -2.6° C and hourly average wind speeds was 3.95 m/s.

Hourly average wind speeds was 3.95 m/s. The highest hourly average wind speed was 18.4 m/s (28.01.2020). The highest 10-min average, with 19.23 m/s was also recorded on 28.01.2020. The predominant local wind direction during the observation period was from the NE (**Figure 3-2**). The highest wind speeds measured came predominantly from NE-E. All wind speeds over 10 m/s came from NE-E. Almost no wind came from NW-N. The wind direction in January was more varied with a higher frequency of winds from WSW **(Figure 3-3**).

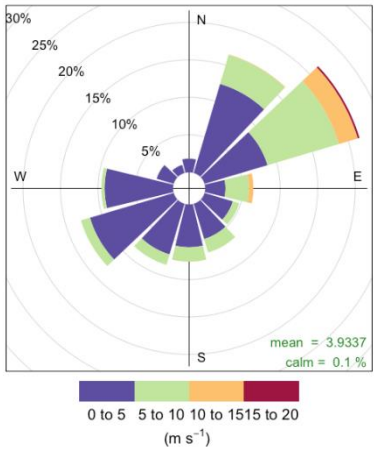

Figure 3-2: Wind rose showing the frequency distribution of hourly average wind data from the AWS for the monitoring period at Kvannberget

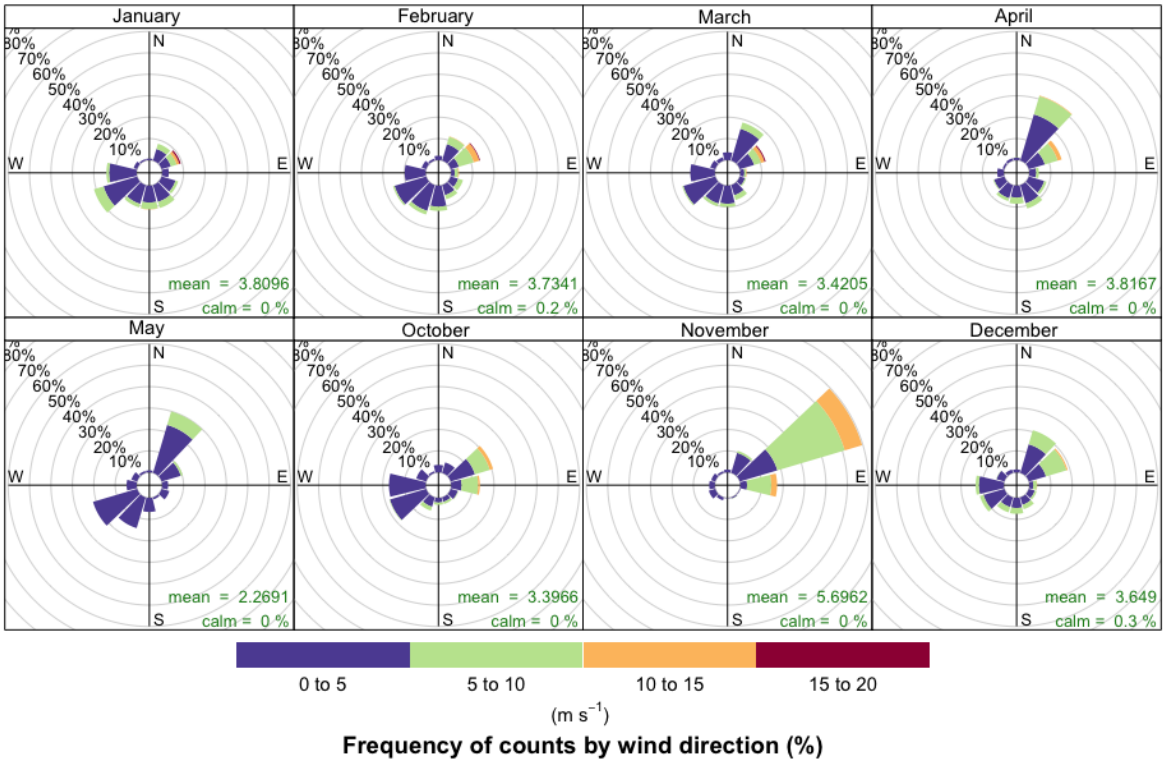

Figure 3-3: Wind roses with the frequency distribution of wind speed counts by wind direction per month. November had the highest frequency of wind speeds above 5 m/s. January had a higher frequency of winds above 5 m/s from the WSW than the other months. Note that October, November and December preceded the other months.

No wind data was gathered in the periods 07.12-10.12.19 and 22.02-25.02.20. There was a slight indication that the lowest temperatures (below -8 degrees Celsius) occur during periods with wind from the North East. No correlations was found between air pressure and wind direction.

The quality of the snow depth measurements was questionable. On several occasions the snow pack was measured to be almost as high as the distance from bare ground up to the sensor. The snow depth was also shown to rapidly increase over short time intervals that did not necessarily coincide with precipitation measured at Sognefjellet. After February the snow depth average was around 45cm, higher than the snow depth observed during field work 06.03.

3.2. Image analysis

Table 2: Overview of the total number of images captured by the five cameras. Two of the cameras failed during the monitoring period.

	Cam 1	Cam 2	Cam 3	Cam 4	Cam 5
Number of images	1239	1838	4323	4496	2226
Failures			15.04.2020 – 12:08	19.10.2019. Fixed 06.03	

A total of 14 122 images were captured by the five cameras. Two of the cameras failed during the monitoring period (**Table 2**). Cam 3 stopped in the middle of April due to an unknown error. Cam 4 took a picture every minute after installation 16.10.2019 and the battery was depleted within four days. The 3 Uovision UV565HD cameras had issues with white balance and many images ended up with a purple hue. This issue was not present with the 2 Uovision UM785-4G cameras. Both camera models overexposed images under bright, sunny conditions.

Cam 2 provided the best view of the control area. 178 of 1838 images were of sufficient quality that measurements of cornice displacement could be made. 152 measurements of horizontal and 142 of vertical displacement were filtered out due to small variations between timeframes to avoid including displacement that could be a result of measurement accuracy.

Figure 3-4: No cornice accretion occurred during October and November. Images from Cam 2. From the left: 26.10.2019, 02.11.2019, 19.11.2019.

The end of October saw several minor snowfalls that quickly melted away (**Figure 3-4**), partly in combination with insolation during the afternoon. Snowfall 30.10.2019 signaled the start of the annual snow cover. Foggy conditions with no visibility arose on 04.12.2019 and lasted until 10.12.2019. Precipitation during the night of 13.12 led to the first signs of cornice development. Cornice accretion could be seen at the location of the reference cornice, as well as a small cornice developing on snow piled up between wind baffle 3 and 4 (**Figure 3-5**).

Figure 3-5: The first accretion event could be seen 14.12.19 (pictured in the middle). A cornice developed in the reference area as well as on the outcrop between baffle 3 and 4. Images from Cam 2. From the left: 10.12.2019, 14.12.2019, 22.12.2019

The cornice in the control area went through cycles with accretion and deformation, until temperatures started to rise 19.12.19 and the snow cover started to decrease. The warm period was over by 22.12.19. Precipitation on the 28.12 led to a slight increase in cornice size, before it started deforming with temperatures above freezing 29.12.19 The lack of daylight hours meant that only 3 pictures had adequate visibility.

Several precipitation events during January led to a visible increase in snow depths but no apparent cornice growth. Snow depths sunk with temperatures above freezing 17.01.20, and

the snow cover had significantly decreased by 21.01. Visibility was low in many periods of January and daylight was not sufficient for accurate measurements of the cornice structure. No apparent growth was observed during this period.

Figure 3-6: Images from cam 2 from morning to afternoon on 09.02. Precipitation with winds from the North-East was observed during the night. Drifting could be seen at 11:00 and the apparent cornice structure was visible at 15:00 (image on the right).

Heavy snowfall was visible on the cameras during the night of 09.02 with winds blowing towards the west. Snow drift was visible during the day and the cornice structure grew at a steep inclination on the leeside of the cliff **(Figure 3-6**). Between 09.02-13.02 visibility was low. Sastrugi had formed by 13.02. showing signs of wind blowing up/against the cliff. No sightings of the cornice were obtained between 15.02-25.02. The images taken in this period reveal foggy conditions or a camera lens covered in snow.

Figure 3-7: A new cornice structure was visible in the reference area on images from 25.02. Images from cam 2 showing drift events 25.02.20 (to the left) and 26.02.20 (to the right).

Visibility cleared up 25.02 revealing a new cornice structure in the control area (**Figure 3-7**). The cornice structure kept growing the following day before the cornice lip started deforming 27.02.

A cornice developed again between wind baffle 3 and 4 28.02. Cornice accretion was quickly followed by deformation.

Figure 3-8: Images from Cam 2 taken 22 hours apart showing an increase in horizontal extent of the cornice in the reference area as well as the development of a cornice structure between baffle 3 and 4. On the left: 29.02 13:00. On the right: 01.03 11:00.

There was more snowfall during the night of 29.02 and subsequent drifting 01.03. The precipitation and drifting contributed to increasing snow depths and both cornice structures experienced substantial growth during the night and morning hours (**Figure 3-8**). Precipitation during nighttime 04.03 led to even further growth of the cornices. The cornice started deforming hours after the drifting ended and continued until 10.03.

Figure 3-9: By 15.03 the cornice face had almost deformed enough to create a roll cavity (red circle). Images from Cam2 09.03 (left) and 15.03 (right).

The leading edge showed signs of rounding 09.03 following a period with warmer temperatures. The cornice roof on both the structures grew again 10.03. The cornice face on the control cornice had deformed to such an extent that snow did not accumulate on the previous leading edge. Further rounding of the leading edge was visible 11.03 as temperatures increased. Sastrugi formation on the snow surface indicated that winds were blowing from North East –

East. Deformation continued until 15.03. The cornice face had now almost deformed enough to create a roll cavity (**Figure 3-9**).

Figure 3-10: 16.03 (left): Sheet growth on the cornice in the reference area, 18.02 (middle): Sastrugi depict a winds blowing against the ridgeline, and 21.03 (right): The cornice structure became rounded with temperatures above freezing and insolation. Images from Cam 2.

Drifting 16.03 led to an increase in snow depth and cornice accretion in the form of sheet growth **(Figure 3-10**). The unsupported sheet rapidly began deforming. Sastrugi seen in pictures 18.03 depict winds blowing against the cliff. The cornice structure became more rounded with temperatures above freezing and insolation. Some accretion occurred during nighttime 25.03, but daytime warming led to a slight reduction in cornice size. Images show signs of wedge growth 29.03 but it could not be determined due to overexposure of images. Only one image was captured during daylight 30.03, revealing a slight accretion event.

Figure 3-11: Increasing temperatures and insolation rapidly lead to a decrease in the snow cover. Images from Cam 2. 15.04 (left) and 05.05 (right).

Images from the start of April indicate periods with winds blowing towards the ridge, as well as an increase in snow depth and deposition of snow at the cornice root. Sastrugi 12.04 shows signs of wind blowing towards the ridge are showing but there also seems to be some increase in cornice size. Precipitation during the night of 15.04 increased snow depth but did not lead to

cornice accretion. Cam 1 was covered in snow from 14.-18.04 as more snow deposited at the cornice root. Snow depth rapidly decreases until 26.04 with many days of insolation and high temperatures. Increasing temperatures and insolation gradually reduced the snow cover and the size of the cornice (**Figure 3-11**). The camera struggled to use correct exposure during periods with insolation and many pictures are overexposed during daytime in this period.

Figure 3-12: The snow cover had been notably reduced by 05.05.20. Note the bare ground around the closest baffle.

3.3. Meteorological conditions during cornice development

16 events of cornice accretion could be visually identified from November 2019 to May 2020. The cornice started developing in December and experienced periods of growth until the middle of April. 21 measurements of horizontal growth and 31 measurements of deformation could be established.

16 drift events could be precisely timestamped based on images. On 12 of these images the snow was visually blowing out over the cliff, from this point referred to as accretion conducive drift. 3 of the events had snow blowing against the ridge. 4 events could only be accounted to be happening within 2 hours (the time since the last image) based on cornice accretion.

The mean temperature during accretion conducive drift events was -6.61° C (min. -0.15°C, max: - 10.37°C). Mean wind speed was 10.26 m/s (min 5.32, max 15.13) with mean wind direction from 74.54 (min 45.86, max 118). The meteorological values corresponding to each drift event is summed up in **Table 3**. For events that could be determined within 2 hours the mean temperature was -3.45°C (min -6.47°C, max -1.31°C), mean windspeed 10.22 m/s (min 6.45, max 13.17) and mean wind direction 70.18° (min 52.98°, max 84.19°).

Table 3: Hourly averages of meteorological data with accretion conducive drift visible on images. 12 events could be precisely timestamped.

Meteorological measurements during accretion conducive drift events			
Date and time of event	Temperature	Wind Speed	Wind Direction
09/02/2020 09:00	-0.29	7.73	113.37
09/02/2020 11:00	-0.15	6.33	118.05
25/02/2020 09:00	-9.86	NA	NA
25/02/2020 11:00	-9.42	NA	NA
26/02/2020 09:00	-10.11	6.79	68.76
26/02/2020 15:00	-9.03	5.32	47.41
26/02/2020 17:00	-10.33	8.01	45.86
29/02/2020 11:00	-6.78	14.10	67.47
29/02/2020 15:00	-5.32	13.92	82.82
29/02/2020 17:00	-5.69	15.13	62.80
01/03/2020 09:00	-6.56	14.32	70.37
16/03/2020 07:00	-5.80	10.94	68.50
Mean	-6.61	10.26	74.54

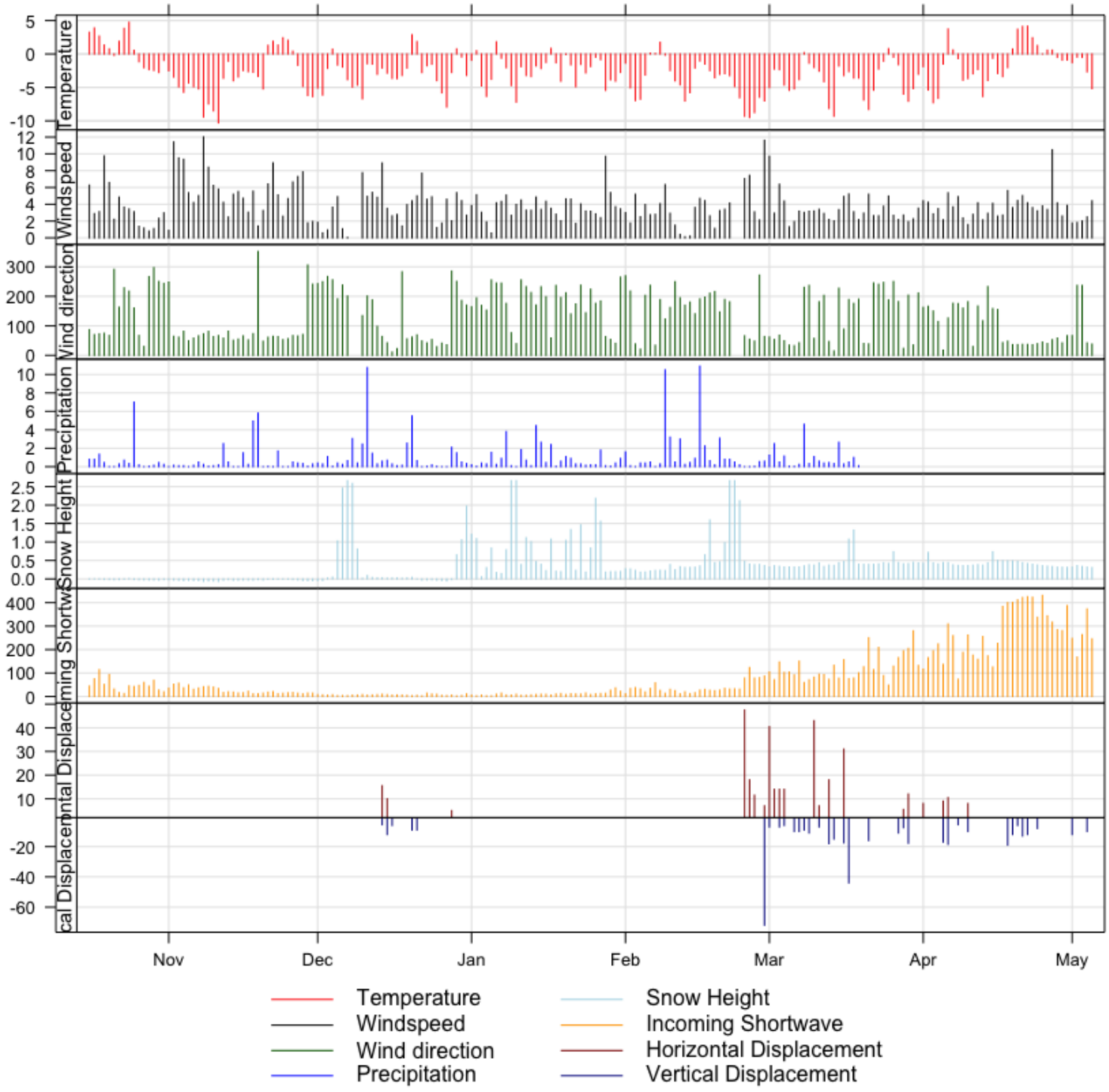

Figure 3-13: Daily average meteorological data and displacement measurements.Precipitation measurements (mm) were collected from the station at Sognefjellet. The other meteorological variables were collected by AWS. Displacement measurements are given in pixel distance and are only relative measurements. Snow height measurements showed sudden increases in snow depth.

Inspection of the 5 hour average conditions preceding an accretion event shows, with the exception of the event 09.02, that accretion occurs during periods with below freezing temperatures. 5 hourly wind speed averages had a minimum at 1.11 m/s and maximum at 13.55 m/s. 10 of the 15 events occurred with a 5 hour average wind direction from North East – East.

Table 4: 5- and 24- hour averages preceding cornice accretion events. The average 24 hour temperature was higher and the wind speed was lower than for the 5 hour average. The average 5 hour wind direction was from the East, while it was from East South-East for the 24 hour average. The missing 24 hour average are due to several events being observed on the same day.

	5 hour average			24 hour average		
Event	Temperature	Wind Speed	Wind Direction	Temperature	Wind Speed	Wind Direction
14.12 15:00	-1.88	9.85	59.63	-2.27	7.75	75.51
28.12 15:00	-2.39	2.06	122.53	-5.00	2.45	141.76
09.02 15:00	0.14	7.17	118.77	-0.30	5.98	159.50
25.02 09:00	-9.70	NA	NA	-8.14	NA	NA
26.02 09:00	-9.13	7.25	57.97	-	-	-
26.02 15:00	-8.90	5.84	54.74	-9.21	7.29	59.98
29.02 07:00	-9.53	10.21	59.19	-	-	-
29.02 11:00	-8.66	13.41	62.18	-	-	-
29.02 15:00	-5.94	13.55	71.27	-7.01	7.88	127.58
01.03 11:00	-6.11	13.42	67.03	-5.23	10.93	61.61
04.03 07:00	-3.92	7.42	49.54	-3.84	6.62	54.34
10.03 13:00	-2.14	5.35	137.06	-1.87	3.33	155.38
13.03 07:00	-7.58	3.07	166.96	-6.53	2.27	161.41
16.03 09:00	-5.39	9.45	63.34	-2.84	4.85	172.13
30.03 19:00	-4.38	1.11	171.70	-5.12	2.28	130.13
12.04 17:00	-7.83	11.29	62.88	-1.49	4.18	175.22
Average	-5.83	8.03	88.32	-4.53	5.48	122.88

24 hour averages are generally warmer, with lower winds speeds from the South East compared to the shorter time intervals (**Table 4**). The average 24 hour temperature was -4.53°C (-0.3°C to -9.21 °C). Wind speeds averaged 5.48 m/s (2.27 m/s – 10.93 m/s) with a 122.88° wind direction (54.34° - 175°C). 24 hour averages were only compiled for individual days, and not for separate events occurring on the same day.

Case study: Accretion 29.02 – 01.03

The cornice structure experienced several accretion events towards the end of February and the start of March. Large accretion rates were visually observed from 29.02 to 01.03 (**Figure 3-14**). Wind speeds began increasing during the night hours of 29.02 as the winds shifted to an North Easterly direction. Hourly wind speed averages were above 10 m/s for a period of 20 hours. Images taken 22 hours apart, at 29.02 13:00 and 01.03 11:00 show a large increase in the horizontal extent of the cornice structure during this period. Horizontal displacement of the leading edge was measured to 78 cm during this time period, resulting in an average hourly displacement of 4.6cm/hour.

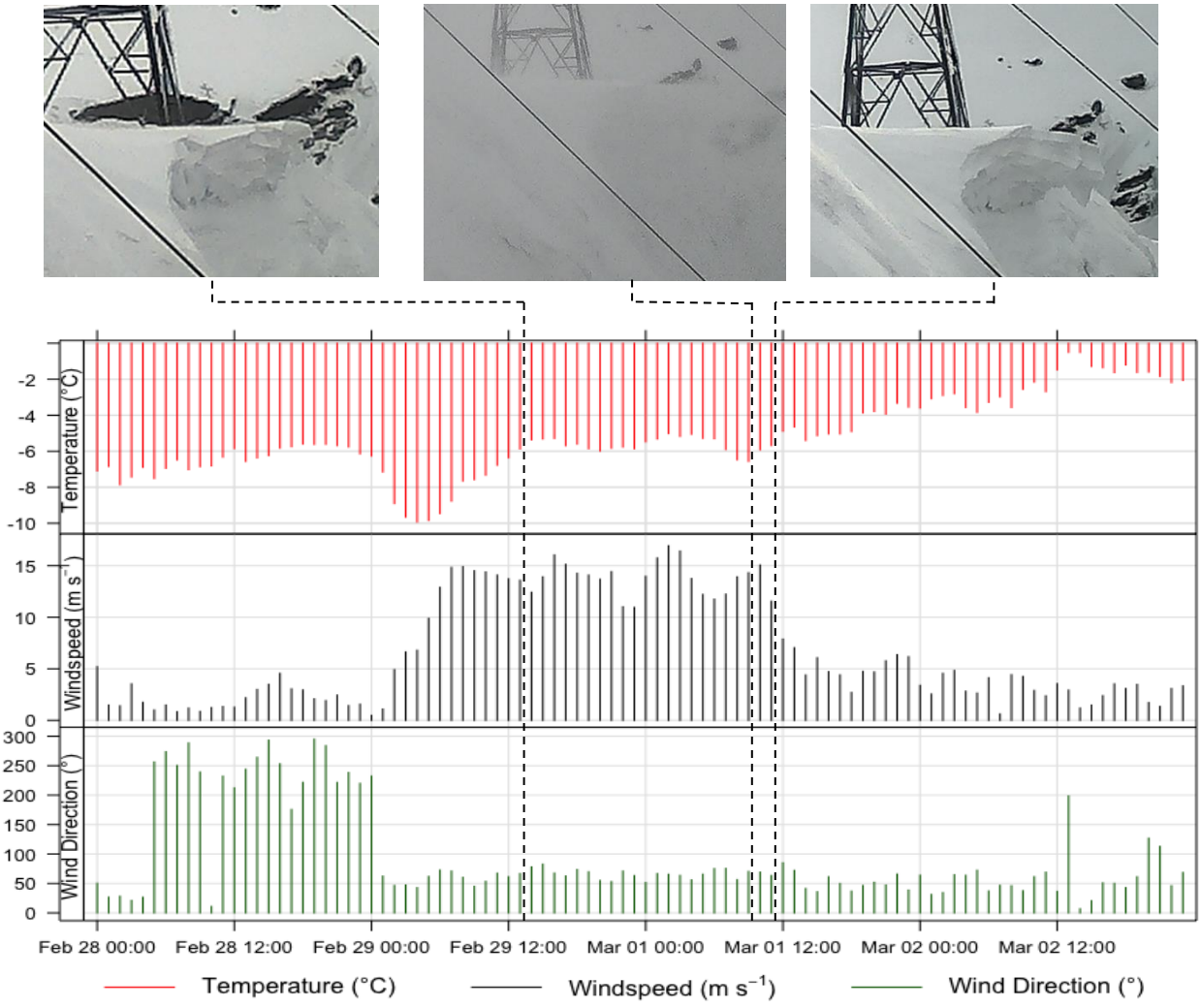

Figure 3-14: Hourly average temperature, wind speed and wind direction for the drift and accretion events observed between 29.02-01.03. Images from Cam 2 of the reference cornice are timestamped (dotted black line). A horizontal extension of the cornice structure was observed from 13:00 29.02 (image on the left)) to 11:00 01.03 (image on the right). The image in the middle shows drifting at 09:00 01.03.

3.4. Comparison of meteorological data from Kvannberget and Sognefjellet

3.4.1 Temperature

The mean daily average temperature measured by the AWS was -2.65 °C and at Sognefjellet it was -6.06°C. Comparison between average daily temperatures show that the temperatures at both the stations fluctuate in the same pattern but temperatures are lower throughout at Sognefjellet (**Figure 3-16**). There was high correlation (**Figure 3-15**) between temperature at the two sites (R>0.83). The daily average temperature at Sognefjellet stayed below freezing from November to mid-April. Minimum and maximum daily temperature at Sognefjellet was -15.69°C and 1.16°C. For the AWS it was -10.29°C and 4.74°C.

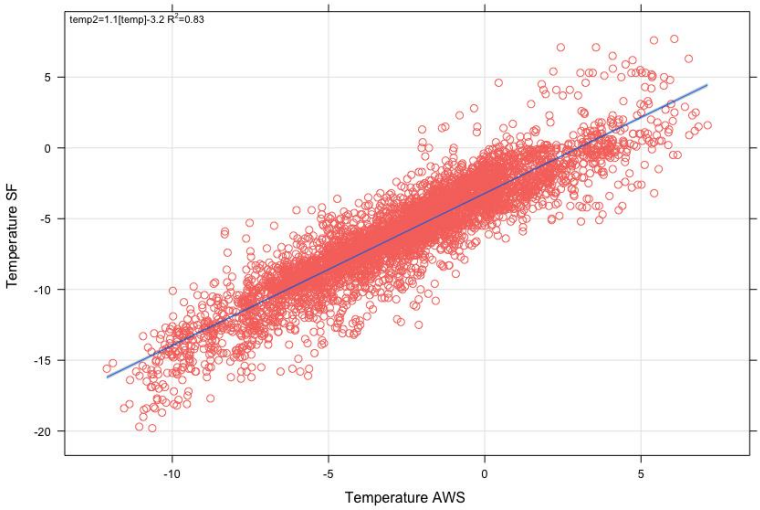

Figure 3-15: Scatterplot show hourly average temperature from the AWS (X-axis) and Sognefjellet (Y-axis). Temperatures between the two station correlated (R>0.83).

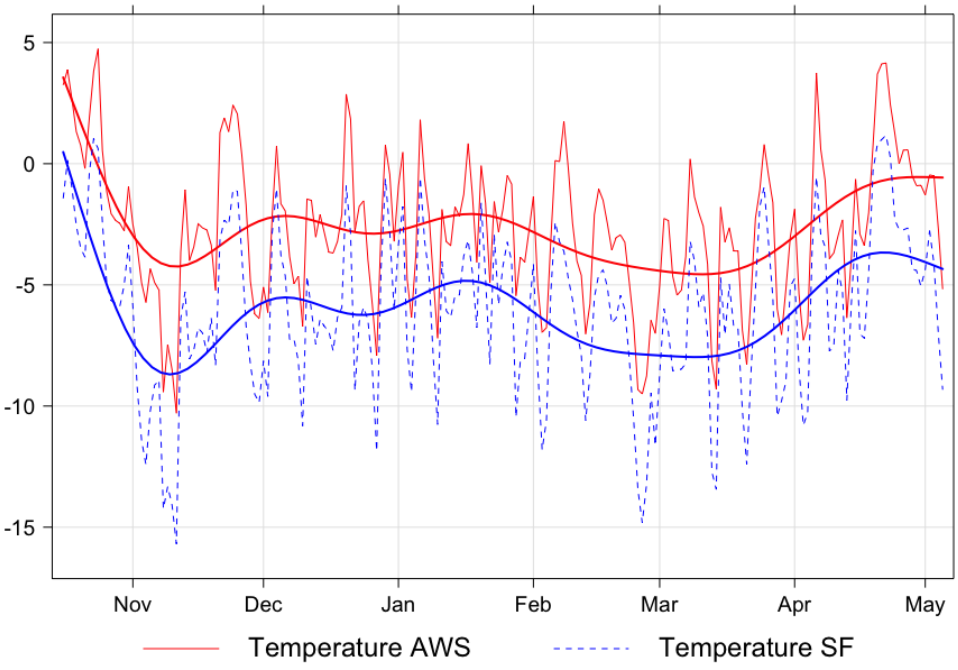

Figure 3-16: Daily average temperature (°C) from the AWS (red) and Sognefjellet (blue) measuring station during the observation period. The same fluctuations can be seen for both stations and the difference is that temperatures at Sognefjellet are lower. A smooth line is plotted for each dataset.

3.4.2Wind measurements

The predominant wind direction was different for the two stations (**Figure 3-17**). Measurements from the AWS show that winds were most common from North-Northeast and that higher wind speeds were most associated with winds from this direction. At Sognefjellet winds were most common from South West-West, also being the direction associated with a higher frequency of high wind speeds. The mean wind speed at Kvannberget was 3.93 m/s. For Sognefjellet it was higher at 5.63 m/s. Sognefjellet had a higher frequency of wind speeds above 10 m/s. The frequency of winds from North North-East was much lower for Sognefjellet than for the AWS. No clear relationships were found for the wind directions at the two stations.

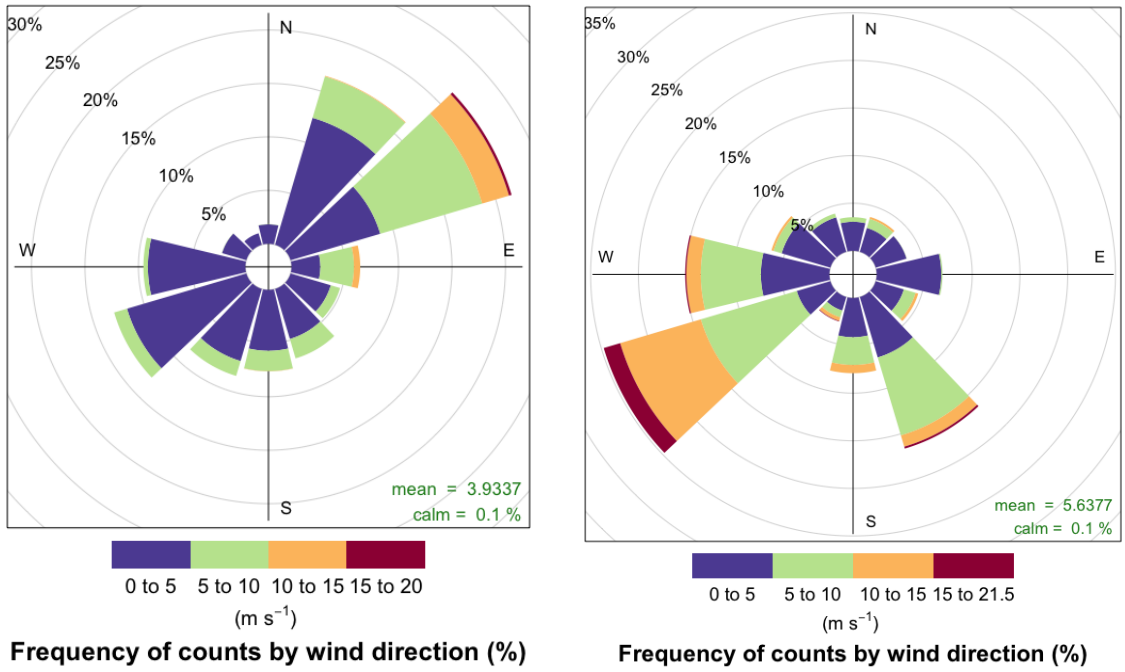

Figure 3-17: Wind rose showing the frequency distribution for wind direction and speed for hourly averages for the AWS (left) and Sognefjellet (right). Wind speeds above 10 m/s at Kvannberget mainly occurred with the predominant wind direction from East North-East. West South-Westerly winds were the most common at Sognefjellet and the direction associated with the highest wind speeds.

To investigate the differences in wind data between measurements from the two different weather stations a frequency distribution showing biases between the two datasets was plotted. The values from the dataset from the AWS was subtracted from the values from the dataset from Sognefjellet. The plot is aimed at showing wind direction biases, but will also show wind speed bias if there simultaneously is a wind direction bias. A situation where the wind at

the two stations had the same direction but differing wind speeds is an example where wind speed bias would not be plotted. The mean windspeed bias was 1.7 m/s showing that hourly winds at Sognefjellet were on average 1.7 m/s higher than at Kvannberget. This can also be seen with the colorcoding on the plot. There is a higher proportion of positively biased wind speeds shown by the red coulours on the plot, compared to the negatively biased wind speeds shown in blue. The frequency of wind speeds being identical at the two locations is low (shown in

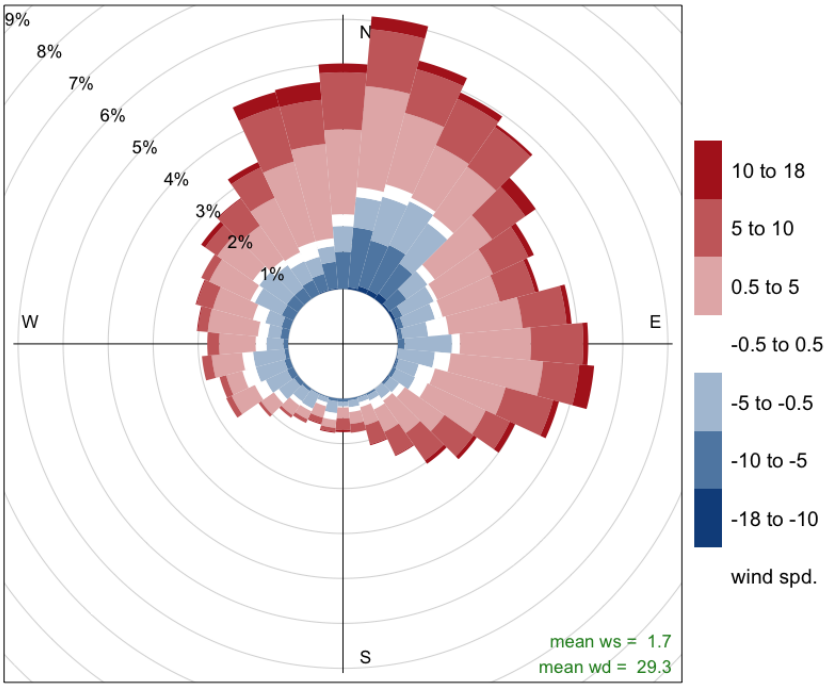

white).

Figure 3-18: Plot showing wind direction biases in polar coordinates between the AWS and the measuring station at Sognefjellet. Note the higher proportion of red color showing that wind speeds were generally higher at Sognefjellet. The blue areas indicate the frequency of periods were wind speeds were higher at Kvannberget.

Figure 3-19 shows the wind at Sognefjellet in periods with wind speeds above 10 m/s at Kvannberget and vice-versa. High wind speeds at Kvannberget are most frequent during periods at Sognefjellet with winds from East and East South-East. The mean hourly wind speeds at Sognefjellet was 7-8 m/s lower than wind speeds at Kvannberget during these periods. The highest wind speeds at Sognefjellet were most frequent from West South-West. These winds most frequently result in winds from the the two southerly quadrants at Kvannberget and lower wind speeds.

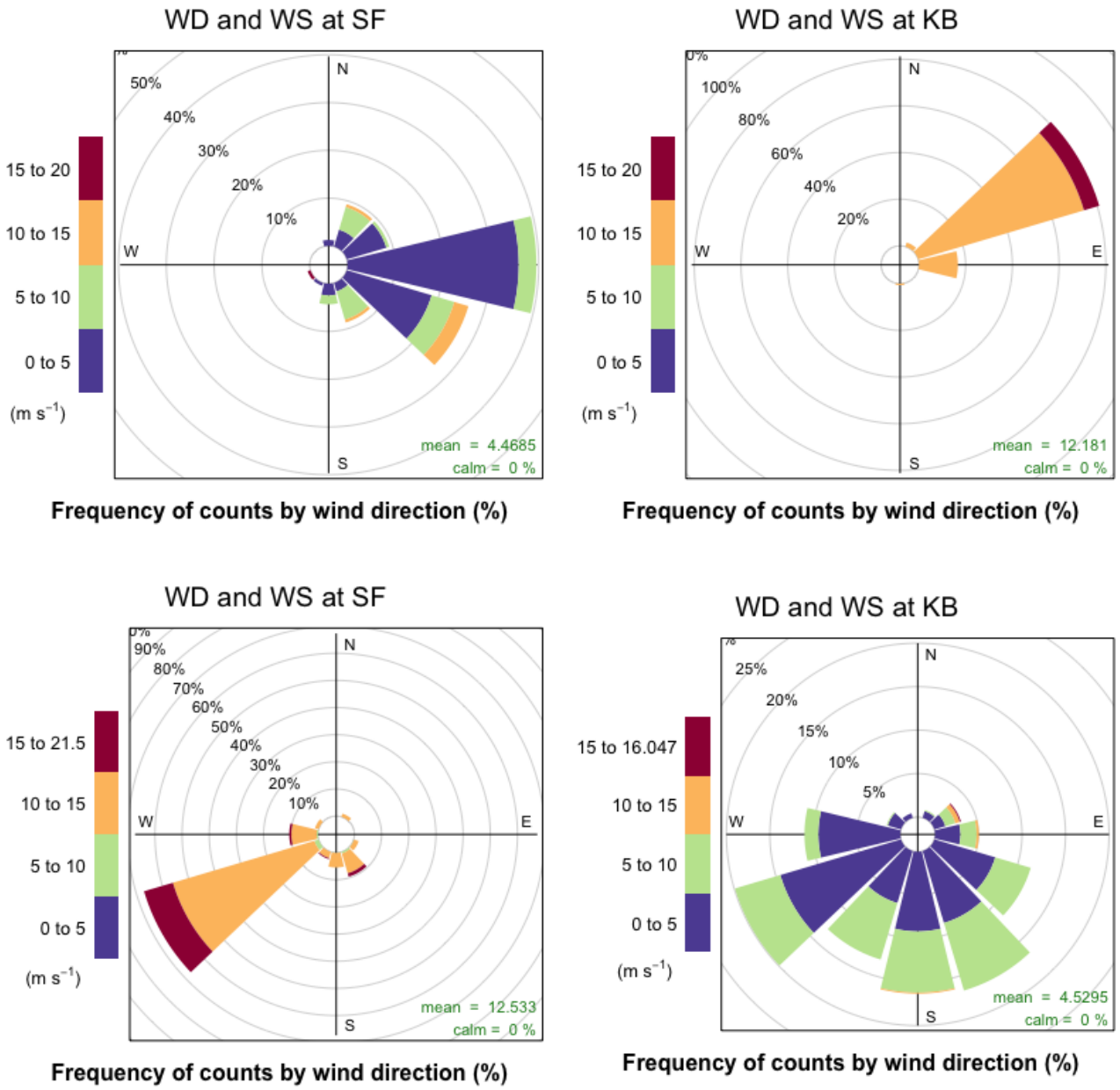

Figure 3-19: Wind roses for conditions at Kvannberget (KB) and Sognefjellet (SF) during periods with wind speeds above 10 m/s. Easterly winds at Sognefjellet results in North Easterly winds at Kvannberget. High wind speeds at Sognefjellet does not result in high wind speeds at Kvannberget. WD: Wind direction. WS: Wind speed.

3.5. Effectiveness of wind baffles

Cornices had developed on many aspects in the surrounding area at the time of field work 06.03. The largest cornice structures were on east faces seen on the other side of the valley. Cornices on north faces were substantially smaller. Cornices had developed along the West-facing cliff in proximity of the study area.

The large continous cornice that had developed 21.02.18 (**Figure 3-20**) did not develop to the same extent during the observation period of the winter 2019/2020 (**Figure 3-21**). The cornice structure in 2018 was continous on the edge of the cliff west of the three southernmost power masts. The cornice structure varied in vertical and horizontal extent along the cliff. No continous cornice structure developed in the area mitigated by the wind baffles during the observation period. There were no signs of cornice formation at the location where the power lines previous had been in contact with the snow. A small cornice developed between baffle 3 and 4.

The cornice structure between the two most southern power masts, used as the reference cornice in this study, grew horizontally and vertically during the observation period. Quantative comparison of this cornice structure between the two years could not be established. By visual inspection the structure seems to be slightly larger in 2018.

Figure 3-20: Aerial image before explosive work was conducted 21.02.2018. A long continuous cornice had developed along the ridge and the powerline on mast 2 had come in contact with the snow.

Figure 3-21:The ridgeline at Kvannberget seen from below. No continuous had developed by 06.03.20. The cornice structure seen between the two masts on the right was used the reference cornice. Image taken during field work 06.03.20

The cornice structure that developed between the two power masts in the middle was situated in the supposedly mitigated area. The first visible accretion event occurred on 14.12.19 when a small cornice lip developed during a period with 8-10 m/s wind from North-East. The lip deformed over the course of December but the snow height towards the edge of the cliff remained. The snow height on the cliff side of the baffles increased even further from the middle of february until a new cornice started developing 28.02.20.

Figure 3-22: Images showing the development of scours around the wind baffles. On the left: The scour was well developed around Baffle nr 1 during fieldwork 06.03. On the right: Image from Cam 4 showing the scour around baffle 1 on the ridge side. Note the increased snow height on the lee side of baffles 3 and 4 in the background.

Scours had develop around the wind baffles during field work 06.03.20 (**Figure 3-22**) and snow depth in near proximity of four out of the five baffles was substantiably lower than that of the surroundings. Snow surface hardness in the sidewalls of the scour was high (1F/P). Upon revisitation of the site 05.05.20 the snow in the near proximity of 4 of the baffles had melted leaving bare ground.

Figure 3-23: Snow had deposited on the lee side of baffles 3 and 4. On the left: The scour around baffle 4 was notably smaller than the other scours. Snow had deposited in contact with the bottom of the baffle. An elevated snow surface can be seen between the scour around baffle 4 and 3 (to the right of the frame). On the left: Snow had deposited on the lee side of baffle 3 (right) and 4 (left). Snow height on the windward side of baffle 4 was notably higher than for baffle 3.

The scour around baffle 4 was notably smaller than around the other baffles and did not extend to the edge of the cliff. Snow had deposited in contact with the bottom of the baffle and snow had accumulated on the ridge side of baffles 3 and 4 (**Figure 3-23**). The scours between baffle 3 and 4 failed to meet, and an wall of hardpacked snow was deposited inbetween the two baffles.

4 Discussion

The discussion is split into 3 sections: The first section covers the meteorological controls of cornice growth at Kvannberget and a comparison between meteorological conditions at Kvannberget and Sognefjellet, the second covers the effectiveness of the wind baffles, and the third covers how climate change will impact future cornice development.

4.1. Meteorological controls of cornice growth at Kvannberget

Cornice development at Kvannberget reinforces the preexisting models of cornice dynamics developed in earlier studies (e.g. Hancock et al., 2020; McCarty et al., 1986; Montagne et al., 1968; Seligman, 1936; Vogel et al., 2012). These models depict that cornice accretion occurs through relatively discrete weather events. The structures rapidly begin to deform under the influence of gravity and meteorological factors before collapsing or melting at the end of the snow season.

The cornice at Kvannberget accreted during or days after snowfall with winds roughly perpendicular to the ridgeline and mean wind speeds around 10.26 m/s. The observed cornice accretion was associated with incremental growth. The cornice grew as a result of drift events with a duration of a few hours. Several drift events were seen in sequence on the same day increasing the daily accretion, separated by periods with no apparent drifting. Continuous drift events over longer timespans were not observed.

To determine the meteorological conditions conducive with cornice accretion, hourly weather data that correlated to images with visible snow drift were investigated. A total of 12 cornice inducive drift events were observed. 5 hour and 24 hour averages were compiled to investigate the weather preceding the events. The longer time intervals smooths out variability in wind and temperature measurements and may fail to describe the combination of meteorological conditions that result in drifting at the site. In contrast shorter time intervals fail to capture the typical duration of an storm event that might lead to accretion.

One example of image intervals and 5-, and 24- hour averages failing to depict weather can be seen on the accretion event 30.03. The exact timing of the event cannot be determined as 34 hours separate observations. The 5 hour averaged wind speed preceding the last image (taken

at 19:00) is 1.11 m/s, significantly lower than threshold wind speed. The accretion event most likely occurred during a small timeframe in the night when North Easterly winds with speeds around 5 m/s were present.

Hourly average wind direction measurements show that accretion was associated with winds blowing relatively perpendicular to the ridgeline at Kvannberget. These drift events occurred with winds from the North East to South East (45-118°). If the two drift events 09.02 are excluded the wind direction was from 45-82°, with a mean of 64.2°. The mean of 5 hour and 24 hour averages of wind direction preceding accretion events was 88.32° and 122.88° respectively. The 5 hour average had a wind direction that ranged from 54-171°. For the 24 hour averages the range was from 54-175°. Kobayashi et al. (1988) observed that cornice direction distribution could deviate from the main wind direction and argued that surface winds chooses the shortest route across the terrain, which would be perpendicular to the ridge direction. The range in wind direction seen during accretion at Kvannberget could be a result of this phenomenon . The AWS was placed further back from the ridge and did not measure wind direction directly at the ridgeline.

The mean wind speed for visible drifting events was 10.26 m/s. 5- and 24 hour averaged wind speed was 8.03 m/s and 5.48 m/s, respectively. These wind speeds are slightly higher than the hourly average wind speed of 8 m/s that Vogel et al. (2012) observed during accretion events on Svalbard and the 7 m/s observed by Montagne et al. (1968) at Bridger Ridge, Montana, USA. With the assumption that accretion is most pronounced around the time that drifting is visible in the images, this could indicate that cornice formation is a result of sufficiently high wind speeds occurring in combination with winds from a distinct direction over a short time interval. Cornice accretion at Kvannberget could be more independent from storm events than the cornices observed by Vogel et al. (2012). The cornice on Svalbard was more exposed to synoptical weather conditions located at the top of a plateau than Kvannberget situated towards the bottom of the catchment area.

Accretion occurred with temperatures close to 0°C. Temperatures were above freezing in the days before the event 09.02. A nighttime decrease in temperature resulted in precipitation in

the form of snow. Drifting without visibly signs of ongoing precipitation ensued at 09.00 and 11.00, with a temperature of -0.29°C and -0.15°C respectively. Hourly average wind speeds for these events was 7.73 m/s and 6.33 m/s. The temperature rose above freezing again at 14.00. Continued accretion was not observed after 14.00 even though the wind speed and direction remained similar to the ones observed earlier in the day. Vogel (2010) also observed accretion events with temperatures close to 0°C. These events were attributed to ongoing snow fall and not to drifting of the preexisting snow surface.

The halt in accretion after the temperature rose at 14.00 might suggest that wind speeds at were not sufficient in mobilizing snow particles from the preexisting snow surface that had previously been subject to above freezing temperatures for several days. The newly fallen snow available for transport might have already been eroded away at this point or increased temperatures might have led to enhanced bond formation, increasing the wind speed required for transport (McClung & Schaerer, 2006).

The accretion event on 09.02 resulted in the development of a structure at a steep inclination on the lee side of the ridge. It is uncertain whether this structure can be classified as a cornice or if it's a result of the formation of a wind slab. It shows signs of a cornice face and does not have support from underneath. It could be an example of vertical accretion described by Montagne et al. (1968) where the growth occurs vertically and not horizontally. The field of view of the camera and image quality did not allow for investigations of the angle of the accretion face and determination of the accretion type.

Sheet accretion was observed 16.02, as a thin horizontal sheet extended out from the cornice structure. Montagne et al. (1968) described sheet accretion as a growth type that occurred under conditions with particularly effective grain to grain adhesion with a rich supply of stellar crystals. The snow crystal type leading to the development of the sheet could not be identified at Kvannberget. The hourly average temperature at the time of visible drifting was -5.8°C. Grain to grain adhesion depends on the liquid water content of the snow crystals (Heil, Mohammadian, Sarayloo, Bruns, & Sojoudi, 2020) and the air temperature (Szabo & Schneebeli, 2007). Szabo and Schneebeli (2007) showed that sintering, the bond formation between snow

crystals, can occur within milliseconds but that the sintering force will be higher at temperatures close to 0°C. Sintering was strong enough to support the sheet that formed 16.02 during drifting but due to the lack of support it rapidly deformed within hours of formation and started to curl downwards as described by Montagne et al. (1968).

Periods with winds above 5 m/s from North-East East following precipitation events were observed without any cornice accretion during the monitoring period. These periods mainly had temperatures above 0°C, followed a period with temperatures above 0°C or followed periods with winds from a direction not associated with accretion, indicating that the cohesion of the snow surface was high enough that snow crystals were not set in motion by the wind. This was the case for January where no accretion was observed. Visibility was poor for a large portion of the month. The mean wind direction was from the South West but there were two periods with winds from the North East - East.

The observed hourly average wind speed for drift events that could be precisely timestamped was in the range from 5.32 m/s – 15.13 m/s, with a mean of 10.26 m/s (**Table 3**). The lowest wind speed associated with accretion, 5.23 m/s, was measured 26.02. Wind data was not available for the drift events the day before. No usable images were collected in the 10 previous days due to lack of visibility. During this 10-day period 38.9 mm of precipitation was measured at Sognefjellet. Abundance of snow available for transport could have allowed for drifting under lower wind speeds (McClung & Schaerer, 2006).

Growth rates could not accurately be determined. The accuracy of the pixel measurements was not high enough due to insufficient image quality and camera placement. Displacement measures could therefore not be used to quantify accretion and deformation. A camera placement showing the cornice structure from the side would have eased distinguishment of the leading edge from the rest of the cornice structure. The accuracy would be further increased with a contrasting background which could allow for quantitative analysis using a particle image velocimetry algorithm (e.g. Reiweger, Ernst, Schweizer, & Dual, 2009). Accretion rates could have been quantified with a higher spatial and temporal resolution using a terrestrial laser

scanner, e.g. Hancock et al. (2020) who were able to quantify changes in the cornice structure with sub-decimeter accuracy.

Horizontal displacement at of the cornice structure from 29.02 to 01.03 could indicate higher accretion rates than the ones observed in earlier studies. Accretion rates during this period was estimated to be around 46mm per hour. Hancock et al. (2020) observed horizontal accretion rates in excess of 10 mm per hour using a terrestrial laser scanner, but note that these rates were conservatively calculated. The accretion rate was calculated from scans 7 days apart with a total increase in horizontal extension of 3m between the two scans. Accretion rates could therefore have been higher in periods. This is valid for Kvannberget as well, where accretion rates were calculated using images 20 hours apart.

The highest growth rates occurred between the end of February to the middle of March and were associated with the events with the highest wind speeds. Hourly average wind speeds above 10 m/s were measured for the events with the largest horizontal growth of the cornice structure. Higher wind speeds lead to a higher rate of snow transport (Pomeroy & Gray, 1995) enabling higher rates of cornice growth up to a certain point. Wind speeds in excess of 25 m/s will lead to scouring and a decrease in cornice size (McClung & Schaerer, 2006).

The maximum horizontal of the cornice was not reached until march, contradicting the findings of Eckerstorfer et al. (2012), where 90% of the maximum vertical and horizontal extent of a cornice on Svalbard was reached during the first autumn snow storms. On possible explanation is the difference in the size of the source area. The cornice studied on Svalbard developed at edge of a large, flat mountain plateau where snow was readily available for transport. The source area at Kvannberget is significantly smaller. Cornice accretion at Kvannberget could have been limited by the weather conditions during the first winter months and several days with temperature above freezing. Another explanation is that cornice accretion at Kvannberget is driven by local meteorological conditions and that accretion is not driven by general storm events.

4.1.1 Comparison of data from the AWS and Sognefjellet

Air temperature variations between the two stations can be a result of elevation differences, and differences in local surface conditions. The proximity of the two stations should neglect differences due to large scale atmospheric circulations and prevailing weather patterns. The temperatures at the two locations follows the same fluctuations and the difference can mainly be attributed to the difference in elevation between the two stations.

The mean wind direction was different for the two measuring stations. The high frequency of winds from West South-West at Sognefjellet is in line with the general weather patterns of the winter 2019/2020. Complex local wind environments found in mountainous terrain is a result of the complexity of the terrain. The AWS at Kvannberget, having a higher frequency of winds from East North-East, indicates that the local wind regime is driven by other factors than the general weather patterns. Local wind can be a function of terrain-induced flow variations.

To investigate whether strong winds at Sognefjellet result in strong winds at Kvannberget wind roses of events with wind speeds above 10 m/s were created (**Figure 3-19**). Wind speeds at Kvannberget were 7-8 m/s lower than winds at Sognefjellet during these events, and periods of strong winds did not coincide between the two stations.

Winds speeds above 10 m/s at Kvannberget mainly occurred with Easterly wind flow at Sognefjellet, indicating that cold air from the East might contribute to East North-Easterly winds at Kvannberget with wind speeds above 10 m/s. These winds at Kvannberget were more frequent during periods with colder temperatures, but this can also be due to the colder temperatures that are generally associated with easterly winds in this region.

One explanation of high winds speeds at Kvannberget is the occurrence of katabatic flow. A katabatic wind is a gravity-driven downslope flow due to cooling of near surface by radiation and sensible heat fluxes. These winds are often found in narrow valleys in the Western part of Norway (Statens Vegvesen, 2014). The topography around the field site supports this

hypothesis, as the field site is located towards the drainage of the catchment area and fall winds would be routed towards the location with a North-Easterly wind direction (**Figure 2-1**).

No correlation was found between incoming solar radiation or air pressure and wind speed which would typically be the driving factors of a fall wind. The hourly average temperature at Sognefjellet was -9.0 C during periods with strong winds at Kvannberget. Katabatic winds can have a synoptic forcing (Klein, Heinemann, Bromwich, Cassano, & Hines, 2001) and an investigation of synoptic weather conditions during periods of high winds at Kvannberget could reveal a correlation between synoptic weather and the local wind regime at Kvannberget. Such an investigation was beyond the scope of this study.

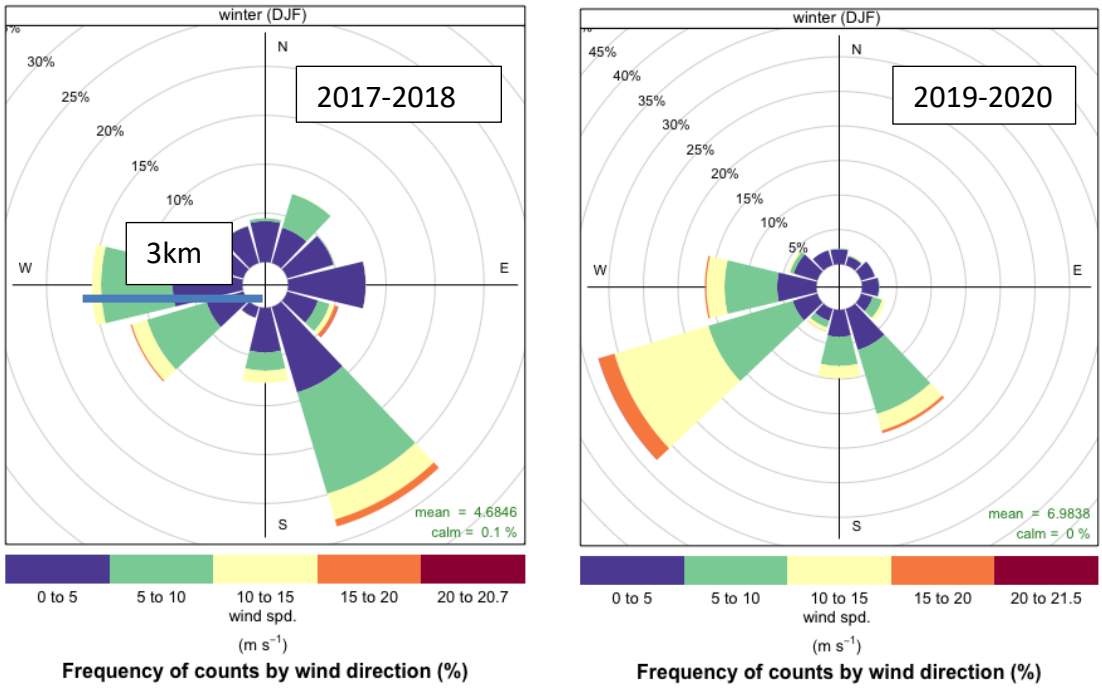

Figure 4-1: Frequency distribution of wind speed and wind direction at Sognefjellet for the winter months of 2017-2018 (on the left) and 2019-2020 (on the right). The predominant wind direction for 2017-2018 was from South South-East. During the same months in 2019-2020 the predominant wind direction was from West South-West.

The predominant wind direction at Sognefjellet during the winter months of 2018 was from South South-East, and also showed a higher frequency of winds from the East than monitoring period (**Figure 4-1**). Easterly flow could have contributed to wind inducive of cornice accretion at Kvannberget and the development of the large cornice structure observed in late February,

2018. This could explain the difference in size of the cornice structure in the control area observed on images between the two years.

The findings indicate that cornice accretion at Kvannberget is a result of complex local meteorological conditions that are difficult to infer from regional weather data without a correlation to synoptical weather conditions.

4.2. Effectiveness of the Wind baffles

Five wind baffles were installed during the fall of 2019 to hinder cornice development in the areas where the power lines previously had come in contact with the snow, which was mainly the area in the proximity of the two middle masts. The effectiveness of the installed wind baffles was evaluated through comparisons with pictures of the cornice structure from earlier years, cornice accretion in the control area, and the influence of the wind baffles on the snow cover.

In 2018 a large continuous cornice developed on the ridge west of the power masts. The horizontal extent of the cornice was variable along the ridge, with large overhanging structures forming to the west of the two southernmost power masts. Further north the cornice did not exhibit the same overhanging nature, but the snowpack had a large horizontal extent.

A large, continuous cornice did not develop to the same extent during the winter of 2019/2020. A small cornice developed on the lee side of baffle 3 and 4. Cornice formation in the control area and slopes with similar aspects in the area indicated that conditions inducive of cornice development had been present.

The snow pack surrounding the wind baffles was significantly influenced. Aerial pictures taken 27.02 show that an abrupt decline in snow depth had developed close to the baffles due to increased erosion of the snow pack (**Figure 4-2**). The drop in snow height was continuous between baffles 1-4. Snow had deposited under the mast between the scours of baffle 4 and 5. The cornice in the control area had not reached maximum horizontal extent at this time.

Figure 4-2: Aerial image of the field site taken 27.02.20. A distinct decline of the snowpack can be seen windward of the baffles.

Scours developed around the wind baffles in a variable extent. The most prominent scour was a large horseshoe shaped scour that developed around baffle 1 (**Figure 3-22**). The scour was

approximately 1m deep by 06.03.20 and only a thin layer of snow remained on the ground in the vicinity of the baffle. The width of the scour could not be measured, as the scour continued towards the cliff. Wopfner and Hopf (1963) observed scours 8-10m wide around baffles 3m without a bottom gap, but these were placed within a continuous snow cover allowing quantification of the scour.

The scour around baffle 4 was significantly smaller than the scours around the other baffles. Wind had deposited directly against the bottom of the structure on the windward side. This was not an issue around the other baffles which had larger clearance between the baffle and the windward scour wall. The baffle was located in a slight depression in the terrain which could inhibit proper formation of the eddy fields and turbulence that lead to erosion around the structure. The baffles at Kvannberget do not have a bottom gap which should facilitate scouring to the ground (Hopf & Bernard, 1963).

The baffle height was adequate for the snow cover height and the baffles were not at risk of being completely covered in snow (Hopf & Bernard, 1963), which would be more likely for baffles placed in location less exposed to continuous wind. Cornice prevention has been found to be successful for baffles with and without bottom gaps (Campell, 1955; Wopfner & Hopf, 1963) as the formation of the eddy zone and leeward transport of snow is the most important feature. Hopf and Bernard (1963) recommended bottom gaps up to 1m and a maximum baffle height of 3m for cornice prevention but do not provide any explanation as to why.

Wind conditions is expected to be similar for all the baffles indicating that the placement of baffle 3 and 4 is less optimal than the other placements. The terrain on the ridgeward side of these baffles has lower declivity than the terrain on the ridgeward side of the other baffles. A rocky outcrop extends several meters westwards of baffle 3 and 4 (**Figure 4-3**). Snow that deposited on this feature during the winter constituted the foundation for the small cornice that formed. A more ridgeward placement of baffles 3 and 4 would place them closer to/in direct contact with the cornice root, as recommended by Hopf and Bernard (1963).

Figure 4-3: Images from Cam 1 and Cam 3 showing the position of the rocky outcrop (red arrow) ridge ward of baffle 3 and 4. A small cornice developed at this location during the monitoring period.

The small cornice that was observed between wind baffle 3-4 is situated between two of the power masts. In a winter season with meteorological conditions inducive of more extensive cornice accretion, a larger cornice might develop in this area but because of its location it would probably not constitute a problem because of the placement in the middle of the two power lines (**Figure 4-4**). Due to the inclination of the slope the horizontal extent of the cornice would be limited by the inclination of the lee slope and a lack of support (Montagne et al., 1968).

Figure 4-4: The field site seen from the West. The red arrow indicates the area where a small cornice developed during the observation period. This area is situated between two of the power masts and an increased horizontal extent would not constitute a problem for the power lines.

The location of the root of the cornice structure that developed in 2018 could not be established through visual inspection of images and the placement of the baffles in relation to the cornice root could not be verified. The baffles are placed in line with the power masts on a relatively flat area several meters from the cliff (**Figure 4-5**). Assuming that the cornice root was located around the break in inclination, the baffles are located several meters away from the cornice root. Wopfner and Hopf (1963) recommended that wind baffles aimed at cornice prevention should be placed directly in the cornice root or up to 1m from the edge of the cliff. Results from Kvannberget indicate that a placement further away from the ridge can produce acceptable results if the baffles are placed on small elevated terrain-features with a significant change in inclination on the leeward side, as seen with baffle 1 and 2.

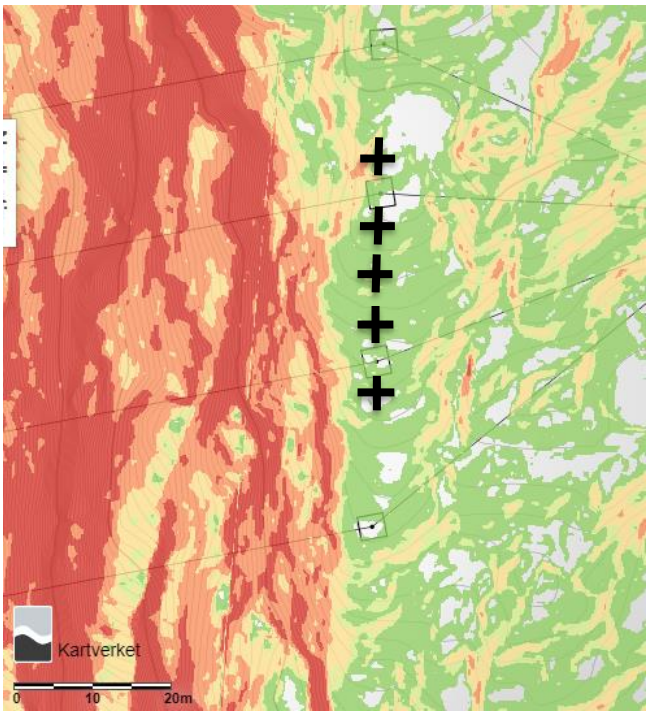

Figure 4-5: Slope angle map of the field site. The black squares show the placement of the power masts. The placement of the wind baffles between the power masts are shown with the black crosses. They are numbered from 1 to 5, with 1 being the most northern baffle.

Visual evaluation of the effectiveness of wind baffles in cornice prevention is sufficient and further investigations of the snowpack around the structures were deemed unnecessary as the results are very visual. Further considerations should be made when using baffles to prevent cornices above avalanche prone slopes as the enhanced snow transport can lead to conditions conducive of snow avalanches. In the case of Kvannberget, transporting snow further down the lee slope does not cause any notable problems. Considerations of baffle placement to prevent cornice formation is mainly limited to whether the aim is to prevent cornice formation entirely or hinder development of a large continuous cornice (Wopfner & Hopf, 1963).

Even though the effectiveness of the wind baffles were only evaluated over one winter season the results are likely to be consistent in other years. Previous studies on the evolution of spatial snow depth distribution in alpine terrain have quantified that there is an inter-annual consistency of snow depth. Trends in snow accumulation patterns over a whole winter season

is similar across observation years, with notable variations only in the absolute snow depth. Storms that occur with wind from the prevailing wind direction produce snow accumulation patterns that are similar to the maximum seasonal snow depth distribution (Prokop & Procter, 2016). These findings are only relevant for locations that have a prevailing wind direction, which is the case for Kvannberget.

4.3. Cornice development in future climate

An increase in average winter temperatures by 4°C by 2100 will influence cornice formation. Accretion events at Kvannberget occurred during temperatures below freezing. Periods were meteorological conditions were conducive of cornice growth, with the exception of temperature, was present during the monitoring period. What separated these periods was the apparent lack of dry, loose snow for snow transport. Precipitation had either fallen as rain or temperatures had increased above freezing preceding the expected drift event indicating that the snow surface bonding was able to resist drifting. Future increases in winter temperatures could lead to a higher frequency of days with temperatures above freezing resulting in a more well bonded snow surface increasing the wind speed required for snow transport. This would limit the amount of snow available for transport and thereby limiting the source material for cornice accretion. Snow pack modeling has shown that rain-on-snow events in north-eastern Switzerland can increase up to 50% with temperatures 2-4°C warmer than today (Beniston & Stoffel, 2016).

With increased temperatures a higher fraction of precipitation will fall as rain, especially in the fall and spring when the average temperature generally is higher. A shorter snow season and shallower snow pack will likely impact cornice development negatively. The monthly average temperature (1961-1990) for Fortun in January and February is -5°C. The measuring site at Fortun is situated at 27 masl., significantly lower the study site at Kvannberget. An increase of 4°C result in average January and February temperatures at Fortun, and by that also Kvannberget, staying below freezing. Interpolated data shows that average annual temperature at Kvannberget was between 0-2°C for the reference period 1971-2000. The observed average temperature from November throughout March was -3.3°C and the projected increased

temperature would have resulted in a much higher frequency of days with temperatures above freezing during the 2019/2020 winter season.

It remains elusive whether wind speeds at Kvannberget will increase in the future. The local and synoptical conditions governing the wind regime at the site have not been identified. It is uncertain how the projected frequency shift towards higher wind speed values and increased maximum wind speeds will affect the location. Periods of high wind speeds at Kvannberget were not associated with periods of high wind speeds at Sognefjellet. An increase of more frequent westerly geostrophic winds during winter (Ruosteenoja et al., 2019) can lead to a lower number of days with wind speeds above 10 m/s at Kvannberget if it leads to a lower frequency of easterly winds at Sognefjellet.

Snow depths at Kvannberget could increase with increasing temperature and higher moisture content (Held & Soden, 2006) up to a point in time when a temperature threshold is reached and a significant fraction of precipitation falls as rain. More intense and frequent atmospheric river events and changes in the North Atlantic oscillation can lead to increased winter precipitation, especially on the South-West coast of Norway (Whan et al., 2020).

A higher frequency of winter storms can lead to increased cornice accretion even though the snow season is shortened, especially in high altitude locations where temperatures remain below freezing, as cornice accretion is a result of discrete events with snow available for transport, temperatures below freezing and sufficient wind speeds in a distinct direction. Past changes in snow depths at Kvannberget were not investigated in this study, but other increases in snow amounts have been identified in other mountainous areas in Norway (I Hanssen-Bauer et al., 2017).

Increases in winter precipitation and wind speeds may generally lead to an increase in cornice accretion. The current and near future might not necessarily be affected by increasing air temperatures as cornices develop at higher elevations where precipitation primary will occur as snowfall. However, it is likely that increased days with temperatures above freezing and an increase in days with rain-on-snow will lead to a decrease in the number of days where snow is readily available for transport (especially at the head and tail of the winter season). The

horizontal and vertical extent of cornices might not be affected by a shorter snow season as they have been observed to reach 90% of their size within the first snow storms of the season (Eckerstorfer et al., 2012).

4.4. Uncertainties and limitations

The experimental design successfully captured visual evidence of cornice accretion that could be related to local meteorological conditions. The resulting interpretations are limited by several factors. Determination of whether cornice accretion was the result of a single drift event, or a composite of multiple events was not possible. Accretion occurring during periods with low visibility, during the night, or between image intervals cannot be identified. The number of accretion and drift events described is inherently a minimum value. Apart from periods with sustained visibility issues, the average temporal gap between images was rather low (sub 24-hours) and accretion and drift events that were not recorded likely occurred in a response to similar meteorological conditions. The accuracy of the accretion rates could not be calculated.

The planned installment of reference stakes could have provided more accurate measurements. However, the rates observed were 4-5 times higher than accretion rates identified in earlier studies and likely outweighs the inaccuracies, indicating that cornice accretion can accrete at higher rates than previously observed. Regular scanning the cornice with a terrestrial laser scanner would have allowed a more precise quantification of accretion rates during periods of cornice growth.

Precipitation measurements were not available at Kvannberget and measurements from Sognefjellet, 10,5 km away and at approximately 500m higher elevation, had to be used. It is uncertain how widely precipitation measurements differ between these two locations. The increased elevation of Sognefjellet would likely result in higher amounts of precipitation at this location (Grünewald, Bühler, & Lehning, 2014). Precipitation gauges are known to undercatch, especially for solid precipitation, and in wind exposed areas in Norway gauges have in some cases been found to have a measurement accuracy below 50% when measuring total winter precipitation (Forland & Aune, 1985). It is not known whether precipitation measurements from Sognefjellet are corrected for this effect. With around 10km separating the two locations it is

reasonable to assume that precipitation events at Sognefjellet coincides with precipitation at Kvannberget. Exact values of precipitation has not been used in the study and therefore the uncertainties tied to the elevation difference and undercatchment are considered acceptable.

The analysis was focused on a single cornice structure, constraining how widely the results can be extrapolated. On the other hand, the fields site resembles terrain and cornice systems in many mountainous environments. Cornice development at lower latitudes may differ from the results in this study, where diurnal variations in temperature and radiation may influence cornice dynamics in ways not seen at Kvannberget.

5 Conclusion

5.1. Investigation of the meteorological controls of cornice growth at Kvannberget

Cornice accretion at Kvannberget was found to reinforce the existing conceptual models of cornice development (e.g. Kobayashi et al., 1988; Montagne et al., 1968; Vogel et al., 2012). Cornice accretion is governed by site specific wind conditions as a result of distinct drift events with hourly average wind speeds significantly higher than the snow season's average wind speeds. Snow readily available for transport was a prerequisite for cornice accretion. The observed drift events leading to accretion were of limited duration but several drift events could in sequence lead to large increase in the horizontal extent of the cornice structure. Accretion rates were found to be 4-5 times higher than the conservative estimates made by Hancock et al. (2020). The accuracy of the accretion rates results depended on the time interval between images of sufficient quality. Measurement methods with higher spatial and temporal resolution would likely quantify even higher accretion rates. Further insights into cornice accretion could be obtained by installing anemometers closer to the cornice root and comparing them to local wind data.

This study demonstrated the viability of using time-lapse imagery for monitoring cornice development. Despite the dependency of visibility, the images provided insights into accretion events and revealed that accretion occurs during short lived events that could be related to local meteorological conditions. The installment of an AWS at the field site provided valuable information on the local meteorological conditions, an advantage that many project do not have. Future work should involve local measurements of snow depth and snow hardness which could enhance the understanding of how snow drifting and erosion of the snow surface relates to accretion periods.

The local meteorological conditions at Kvannberget were found to be difficult to infer from regional weather data. The local wind regime at Kvannberget deviated from wind data from the weather station at Sognefjellet and periods of high wind speeds rarely coincided between the two locations. Wind speeds above 10 m/s mainly occurred with East North-Easterly winds at Kvannberget during periods with Easterly winds with lower wind speeds at Sognefjellet

indicating that high wind speeds at Kvannberget might be a result of fall winds. To gain a better understanding of the weather systems driving cornice accretion at Kvannberget, drift events need to be correlated to synoptical weather conditions.

5.2. Evaluation of the effectiveness of the installed wind baffles

The five installed wind baffles were found to proficiently mitigate the development of the continuous cornice that previously had developed along the ridge. The results should be consistent for upcoming snow seasons due to the fact that the snowpack in an area of a prevailing wind direction usually shows inter-annual consistency (Prokop & Procter, 2016). The snow pack surrounding the baffles was significantly influenced as scours formed around the structures. The efficiency of the baffles depended on the underlying terrain and the distance to the ridgeline. A small cornice developed ridgeward from the 2 baffles placed furthest away from the break in terrain and scour formation around one of the baffles was hindered by being placed in a small depression in the terrain.

In locations where baffles are used to mitigate cornice development the preferred placement is directly in the area of the cornice root or up to 1m from the break in inclination. The number and spacing of baffles depends on whether the cornice should be prevented entirely or if it sufficient to simply prevent the formation of a continuous structure. When used on cornices overlying avalanche-prone slopes other considerations have to be made on how they affect the underlying slope. Time-lapse imagery with a birds-eye view above a wind baffle can improve understanding of how the scour develops during a winter season and how the erosion process is affected by different wind conditions.

5.3. Climate Change and future cornice development

Cornice accretion occurs as a response to distinct local meteorological events and cornice development will likely be impacted by climate change. Projected temperature increases can lead to a higher frequency of days with temperatures above freezing and limit the number of accretion events. Snow depths at high altitudes can increase in Western Norway in the future due to increased winter temperatures and higher moisture content, a higher frequency of atmospheric river events and future shifts in the North Atlantic Oscillation. Increased winter

precipitation and a general shift towards higher winter wind speeds can lead to an increase in the effective snow depth and higher frequency of cornice accretion events. A shorter snow season might not affect the horizontal and vertical extent of cornices as they can reach 90% of their size within a few snow storms (Eckerstorfer et al., 2012). Wind baffles have shown to be effective at permanently mitigating hazards related to snow cornices and can be a cost-effective tool to reduce risk in a future where natural hazards are more common.

6 References

Aschenwald, J., Leichter, K., Tasser, E., & Tappeiner, U. (2001). Spatio-temporal landscape analysis in mountainous terrain by means of small format photography: a methodological approach. *IEEE transactions on geoscience and remote sensing, 39*(4), 885-893.

Azad, R., & Sorteberg, A. (2017). Extreme daily precipitation in coastal western Norway and the link to atmospheric rivers. *Journal of Geophysical Research: Atmospheres, 122*(4), 2080-2095.

Beniston, M., & Stoffel, M. (2016). Rain-on-snow events, floods and climate change in the Alps: Events may increase with warming up to 4 C and decrease thereafter. *Science of the Total Environment, 571*, 228-236.

Burrows, R., & McClung, D. M. (2006). *Snow cornice development and failure monitoring.* Paper presented at the International Snow Science Workshop, Telluride Colorado.

Campell, E. (1955). Treibschneewände oder Kolktafeln und ihre Anwendung in de Lawinenverbauung. *Bünderwald, 8*(Nr 5).

Christiansen, H. H. (2001). Snow-cover depth, distribution and duration data from northeast Greenland obtained by continuous automatic digital photography. *Annals of Glaciology, 32*, 102-108.

Dexter, L. R., & Cluer, B. L. (1999). Cyclic erosional instability of sandbars along the Colorado River, Grand Canyon, Arizona. *Annals of the Association of American Geographers, 89*(2), 238-266.

Droppo, J. G., & Napier, B. A. (2008). Wind direction bias in generating wind roses and conducting sector-based air dispersion modeling. *Journal of the Air & Waste Management Association, 58*(7), 913-918.

Eckerstorfer, M., Bühler, Y., Frauenfelder, R., & Malnes, E. (2016). Remote sensing of snow avalanches: Recent advances, potential, and limitations. *Cold Regions Science and Technology, 121*, 126-140.

Eckerstorfer, M., Christiansen, H., Vogel, S., & Rubensdotter, L. (2012). Snow cornice dynamics as a control on plateau edge erosion in central Svalbard. *Earth Surface Processes and Landforms, 38*(5), 466-476.

Eckerstorfer, M., & Vogel, S. (2014). Snow cornices and cornice fall avalanches: A short review of current and past research. *The Avalanche Journal, 107*, 54-59.

Forland, E., & Aune, B. (1985). *Comparison of Nordic methods for point precipitation correction.* Paper presented at the Correction of Precipitation Measurements.

Førland, E., Hanssen-Bauer, I., Haugen, J., Hygen, H., Haakenstad, H., Isaksen, K., & Dyrrdal, A. (2016). Background Information for 'Klima i Norge 2100'. *NCCS report, 1*, 50.

Fuchs, v. A. (1954). Modellversuche mit Kolktafeln im Windkanal. [Wind tunnel model tests with baffles]. *Forstliche Bundesversuchsanstalt Mariabrunn. Wien*.

Germain, D., Filion, L., & Hétu, B. (2009). Snow avalanche regime and climatic conditions in the Chic-Choc Range, eastern Canada. *Climatic Change, 92*(1-2), 141-167.

Grünewald, T., Bühler, Y., & Lehning, M. (2014). Elevation dependency of mountain snow depth. *The Cryosphere, 8*(ARTICLE), 2381-2394.

Guan, B., Molotch, N. P., Waliser, D. E., Fetzer, E. J., & Neiman, P. J. (2010). Extreme snowfall events linked to atmospheric rivers and surface air temperature via satellite measurements. *Geophysical Research Letters, 37*(20).

Hákonardóttir, K. M., Margreth, S., Tómasson, G., Indriðason, H., & Thordarson, S. (2008). *Snow drift measures as protection against snow avalanches in Iceland*. Paper presented at the International symposium on mitigative measures against snow avalanche, Egilsstaðir, Iceland.

Hancock, H., Eckerstorfer, M., Prokop, A., & Hendrikx, J. (2020). Quantifying seasonal cornice dynamics using a terrestrial laser scanner in Svalbard, Norway. *Natural Hazards and Earth System Sciences, 20*(2), 603-623.

Hanssen-Bauer, I., Førland, E., Haddeland, I., Hisdal, H., Mayer, S., Nesje, A., . . . Sorteberg, A. (2017). Climate in Norway 2100–a knowledge base for climate adaptation. *NCCS report*, 204.

Hanssen-Bauer, I., Førland, E. J., Haddeland, I., Hisdal, H., Mayer, S., Nesje, A., . . . Ådlandsvik, B. (2015). *Klima i Norge 2100* (2/2015). Retrieved from https://cms.met.no/site/2/klimaservicesenteret/rapporter-og-publikasjoner/_attachment/6616?_ts=14ff3d4eeb8

Heil, J., Mohammadian, B., Sarayloo, M., Bruns, K., & Sojoudi, H. (2020). Relationships between Surface Properties and Snow Adhesion and Its Shedding Mechanisms. *Applied Sciences, 10*(16), 5407.

Held, I. M., & Soden, B. J. (2006). Robust responses of the hydrological cycle to global warming. *Journal of Climate, 19*(21), 5686-5699.

Hewes, J., Decker, R., Wood, P., & Jamie Yount, W. (2008). *Passive Avalanche Defense for a Domestic Transportation Application: The Milepost 151 Avalanche, Jackson, Wyoming.* Paper presented at the 2008 International Snow Science Workshop.

Holle, R. L., Simpson, J., & Leavitt, S. W. (1979). GATE B-scale cloudiness from whole-sky cameras on four US ships. *Monthly Weather Review, 107*(7), 874-895.

Hopf, J., & Bernard, J. (1963). Windbeeinflussende Bauten in der Lawinenverbauung und—Vorbeugung. [Wind Control Structures in Avalanche Defence and Prevention]. *Ökolo gische Untersuchungen in der subalpinen Stufe der Zentralalpen II. Mitt. Forstl. Bundesversuchsanstalt Mariabrunn*(60), 605-632.

Klein, T., Heinemann, G., Bromwich, D. H., Cassano, J. J., & Hines, K. M. (2001). Mesoscale modeling of katabatic winds over Greenland and comparisons with AWS and aircraft data. *Meteorology and Atmospheric Physics, 78*(1-2), 115-132.

Klett, M. (2004). *Third views, second sights: a rephotographic survey of the American West*: Museum of New Mexico Press.

Klett, M. (2011). Repeat photography in landscape research. *The Sage handbook of visual research methods*, 114-131.

Kobayashi, D., Ishikawa, N., & Nishio, F. (1988). Formation process and direction distribution of snow cornices. *Cold Regions Science and Technology, 15*(2), 131-136.

Krasting, J. P., Broccoli, A. J., Dixon, K. W., & Lanzante, J. R. (2013). Future changes in Northern Hemisphere snowfall. *Journal of Climate, 26*(20), 7813-7828.

Laute, K., & Beylich, A. A. (2018). Potential effects of climate change on future snow avalanche activity in western Norway deduced from meteorological data. *Geografiska Annaler: Series A, Physical Geography, 100*(2), 163-184.

Malin, D. (2007). Time-Lapse Photography. In *The Focal Encyclopedia of Photography* (pp. 622-623): Elsevier.

Margreth, S., Jóhannesson, T., & Stefánsson, H. M. (2014). *Avalanche Mitigation Measures for Siglufjörður–Realization of the Largest Project with Snow Supporting Structures in Iceland.* Paper presented at the Proc. International Snow Science Workshop, Banff, Canada.

Martinelli, J. M. (1960). *A look at avalanche control structures in Europe.* Paper presented at the Proceedings, 28th Western Snow Conference 1960.

McCarty, D., Brown, R., & Montagne, J. (1986). *Cornices: their growth, properties, and control.* Paper presented at the International Snow Science Workshop, Lake Tahoe.

McClung, D., & Schaerer, P. (2006). *The avalanche handbook* (3rd ed. ed.). Seattle, Wash: Mountaineers Books.

Mellor, M. (1965). Blowing snow. Cold regions science and engineering part III, section A3c. *Hanover, NH: US Army Cold Region Research and Engineering Laboratory*.

Montagne, J., McPartland, J., Super, A., & Townes, H. (1968). *The nature and control of snow cornices on the Bridger Range, Southwestern Montana, Alta Avalanche Study Center*. Retrieved from

https://www.researchgate.net/publication/37516318_The_Nature_and_Control_of_Snow_Cornices_on_the_Bridger_Range_Southwestern_Montana

Munroe, J. S. (2018). Monitoring snowbank processes and cornice fall avalanches with time-lapse photography. *Cold Regions Science and Technology, 154*, 32-41.

Norsk Klimaservicesenter. (2017). *Klimaprofil Sogn og Fjordane - Eit kunnskapsgrunnlag for klimatilpassing*. Retrieved from https://cms.met.no/site/2/klimaservicesenteret/klimaprofiler/klimaprofil-sogn-og-fjordane/_attachment/12038?_ts=15d9d3d51bf

Parajka, J., Haas, P., Kirnbauer, R., Jansa, J., & Blöschl, G. (2012). Potential of time-lapse photography of snow for hydrological purposes at the small catchment scale. *Hydrological Processes, 26*(22), 3327-3337.

Perla, R. I., & Martinelli, M. (1976). *Avalanche handbook*: US Department of Agriculture, Forest Service.

Pomeroy, J., & Gray, D. (1995). Snowcover accumulation, relocation and management. *Bulletin of the International Society of Soil Science no, 88*(2).

Prokop, A., & Procter, E. S. (2016). A new methodology for planning snow drift fences in alpine terrain. *Cold Regions Science and Technology, 132*, 33-43.

Reiweger, I., Ernst, R., Schweizer, J., & Dual, J. (2009). *Force-controlled shear experiments with snow samples.* Paper presented at the Proceedings International Snow Science Workshop, edited by: Schweizer, J. and van Herwijnen, A., Davos, Switzerland.

Rudolf-Miklau, F., Sauermoser, S., Mears, A. I., & Boensch, M. (2015). *The technical avalanche protection handbook*: Wiley Online Library.

Ruosteenoja, K., Vihma, T., & Venäläinen, A. (2019). Projected changes in European and North Atlantic seasonal wind climate derived from CMIP5 simulations. *Journal of Climate, 32*(19), 6467-6490.

Seligman, G. (1936). Cornices. In *Snow structure and ski fields* (pp. 237-269): Macmillan.

Sillmann, J., Kharin, V. V., Zwiers, F., Zhang, X., & Bronaugh, D. (2013). Climate extremes indices in the CMIP5 multimodel ensemble: Part 2. Future climate projections. *Journal of Geophysical Research: Atmospheres, 118*(6), 2473-2493.

Statens Vegvesen. (2014). *Veger og drivsnø: veiledning [Håndbok V137]* (8272076446). Retrieved from https://www.vegvesen.no/_attachment/305996/binary/963979?fast_title=Håndbok+V137+Vegetr+og+drivsnø.pdf

Szabo, D., & Schneebeli, M. (2007). Subsecond sintering of ice. *Applied Physics Letters, 90*(15), 151916.

Tsanis, I., & Tapoglou, E. (2019). Winter North Atlantic Oscillation impact on European precipitation and drought under climate change. *Theoretical and Applied Climatology, 135*(1-2), 323-330.

USDA Forest Service. (1975). *Avalanche Protection in Switzerland* (Vol. 9): U.S. Department of Agriculture.

van Herwijnen, A., Berthod, N., Simenhois, R., & Mitterer, C. (2013). *Using time-lapse photography in avalanche research.* Paper presented at the Proceedings ISSW.

van Herwijnen, A., & Fierz, C. (2014). Monitoring snow cornice development using time-lapse photography. *Proceedings of the International Snow Science Workshop, 2014, Banff, Canada*, 865-869.

van Herwijnen, A., & Simenhois, R. (2012). *Monitoring glide avalanches using time-lapse photography.* Paper presented at the International Snow Science Workshop ISSW.

Verge, R., & Williams, G. (1981). Drift control. *Handbook of snow: principles, processes, management and use. Toronto, Ont., Pergamon Press Canada Ltd*, 630-647.

Vogel, S. (2010). *Cornice accretion, cracking and failure along with their meteorological controls at Gruvefjellet, Central Svalbard.* (Master, University of Oslo). Retrieved from https://www.duo.uio.no/handle/10852/12668

Vogel, S., Eckerstorfer, M., & Christiansen, H. (2012). Cornice dynamics and meteorological control at Gruvefjellet, Central Svalbard. *The Cryosphere, 6*(1), 157-171.

Webb, R. H. (1996). *Grand Canyon: A Century of Change: Rephotography of the 1889-1890 Stanton Expedition*: University of Arizona Press.

Whan, K., Sillmann, J., Schaller, N., & Haarsma, R. (2020). Future changes in atmospheric rivers and extreme precipitation in Norway. *Climate Dynamics, 54*(3), 2071-2084.

Wopfner, H., & Hopf, J. (1963). Versuche mit Kolktafeln an der Schneeforschungsstelle Wattener Lizum (Tirol) in den Jahren 1950–1955. [Tests with baffles at the Wattener Lizum Snow Research Station (Tyrol) in the Years 1950-1055]. *Forstliche Bundesversuchsanstalt Mariabrunn. Wien*.